

Algorithmic collusion under competitive design

Ivan Conjeaud†

November 2023

Abstract

We study a simple model of algorithmic collusion in which Q-learning algorithms are designed in a strategic fashion. We let players (*designers*) choose their exploration policy simultaneously prior to letting their algorithms repeatedly play a prisoner's dilemma. We prove that, in equilibrium, collusive behavior is reached with positive probability. Our numerical simulations indicate symmetry of the equilibria and give insight for how they are affected by a parameter of interest. We also investigate general profiles of exploration policies. We characterize the behavior of the system for extreme profiles (fully greedy and fully explorative) and use numerical simulations and clustering methods to measure the likelihood of collusive behavior in general cases.

Keywords: Algorithmic collusion, Q-learning, Reinforcement Learning, Multi Agent Reinforcement Learning.

JEL classification: C72, C63

†Affiliation: *Paris School of Economics*, 48 Boulevard Jourdan, 75014 Paris, ivan.conjeaud@psemail.eu

1 Introduction

Algorithms are increasingly used to take decisions on behalf of humans in a wide range of contexts. Delegating to machines allows faster decision making and is now common in retail pricing, stock trading, and auction bidding. Given this prevalence of automatic decision making in economic contexts, competition between algorithms is pervasive. Examples include automated auctions for advertisement spots, in which several algorithms compete to display a commercial on a web page, or the price competition between several firms using automatic pricing on a retail platform. In such contexts, since the economic agents are delegating their decision making power to algorithms, competition between them takes place on the technology. For example, firms using algorithms to trade assets might be incentivized to adopt better performing machines to increase their speed of trading. In this paper, we focus on the competition taking place between algorithm designers delegating their decision making to reinforcement learning algorithms. Among the numerous types of algorithms available to solve a specific task, reinforcement learning, and together with it, its building brick *Q-learning*, is oftentimes a good candidate. It is a type of machine learning in which the machine *learns by doing*, requiring few or even no information about the economic environment, and is thus adapted to a wide range of economic situations.

In our model, two Q-learning algorithms with an ε -greedy policy repeatedly play a parameterized Prisoner's Dilemma. Q-learning is a simple reinforcement learning algorithm that associates to each action a value (the *Q-value*) and relies on a *exploration policy* to select an action in each round. We consider here that the algorithms use a classic ε -greedy policy : in each round, the algorithm selects the action with highest Q-value with probability $1 - \varepsilon$ (which corresponds to *exploiting*) and selects any action with uniform probability with probability ε (which corresponds to *exploring*). We study a *designing game* in which two algorithm designers, *A* and *B*, need to choose an exploration policy, implement it in their respective algorithms and let them repeatedly play a prisoner's dilemma on their behalf. In order to focus on the *limiting behavior* of algorithms, we assume the payoffs of this game are the ones obtained upon convergence. We contribute to the study of interacting Q-learning algorithms by: (i) characterizing the behavior of algorithms when they use extreme values of ε , (ii) proving that every Nash equilibrium in the designing game must feature some cooperative behavior, (iii) investigating the behavior for other parameters and studying other equilibria of the game by using extensive numerical simulations.

Q-learning algorithms have been reported to learn to play cooperation in the long run. To investigate this phenomenon, we use the same framework as Banchio and Mantegazza (2023)[4], who introduced the notion of *spontaneous coupling*. Q-learning algorithms only update Q-values of the action that is played, which is often referred to *asynchronous updating* in the literature. The link between spontaneous coupling and asynchronous updating has been observed

by Asker (2022) [2] as well as by Banchio and Skrzypacz (2022) [5], and formally identified by Banchio and Mantegazza (2023). Because of asynchronous updating, when an algorithm plays cooperation (resp. defection), its opponent’s Q-value of the action it has used increases (resp. decreases) while the other stays still. This simple mechanism explains the alternation of cooperative and non-cooperative phases under spontaneous coupling. Schematically, when both algorithms hold cooperation (C) has a preferred action, the Q-values for both actions tend to increase, though, the one for defection (D) increases, on average, faster. This causes the algorithms to eventually switch to a non-cooperative phase in which D is held as a preferred action. In this non-cooperative phase, Q-values for both actions tend to decrease. When cooperation is not updated frequently enough (*i.e.* when ε is low), the Q-value for action D decreases faster than this for action C , causing both algorithms to be back to a cooperative phase. Banchio and Mantegazza (2023) prove this point formally using a continuous-time approximation when algorithms use the same exploration policy. Since spontaneous coupling disappears for some values of the exploration parameter, a natural question is whether it remains possible when algorithms’ designers compete using the parameters. We are thus interested in the equilibria of the aforementioned designing game.

Most of the known results on algorithmic collusion are simulation based, due to the difficulty of mathematically characterizing the complex interactions of several reinforcement learning algorithms. When a single Q-learning agent is considered facing a stationary environment, convergence to an optimal policy is guaranteed under mere conditions on the learning rates (Watkins and Dayan 1992 [33]). However, when two or more agents interact with the same environment, those convergence guarantees do not hold anymore. Indeed, the “subjective environment” of an algorithm includes another algorithm that reacts to the first one’s behavior, causing non-stationarity (Canese et al 2021 [10]). Thus, in order to investigate the properties of interacting Q-learning algorithms, the use of extensive numerical simulations is necessary most of the time. A few papers provide analytical results though. Banchio and Mantegazza (2023) are able to provide analytical results, however their proof relies on an assumption of symmetry in the initial conditions that we cannot use when considering different exploration policies. Dolgoplov (2024) [15] gives general results on asymmetric Q-learning algorithms repeatedly playing a prisoner’s dilemma. He gives a full characterization of the set of *stochastically stable* states for the algorithms in the cases of ε -greedy and Boltzmann exploration policies. However, stochastic stability fails to characterize the long-run behavior of the algorithms, as shown and explained by Xu and Zhao (2024) [34]. Abusively, stochastic stability characterizes a state of the algorithms (a vector of Q-values) that is attained with positive probability as exploration vanishes to zero *once* the algorithms have reached their stationary behavior. By contrast, in the present article we assume *non-vanishing* exploration and work on the stationary behavior of the algorithms given these exploration policies.

As a first step we analytically characterize the behavior of the algorithms for extreme values of exploration parameters. They correspond to stereotypical behaviors: when an algorithm uses $\varepsilon = 0$, it only plays the action with highest Q-value (it always *exploits*, we refer to it as *greedy*), while when an algorithm uses $\varepsilon = 1$, it uniformly randomizes between the two actions (it always *explores*). When at least one of the algorithms uses one of these extreme parameters, the behavior of the system becomes easier to analyze. We investigate three cases: (i) when one of them uses $\varepsilon = 1$ (i.e. explores all the time) (ii) when one of them uses $\varepsilon_A = 0$ and the other uses $\varepsilon_B > 0$ (i.e. when *A* only exploits) and (iii) when both use $\varepsilon = 0$. In the first two cases, we show that spontaneous coupling disappears, whereas in the third it remains possible. We then leverage these results in order to deduce some properties of the Nash equilibria. First we show that $(\varepsilon = 0, \varepsilon = 0)$ is a Nash equilibrium of the designing game. As a unilateral deviation from this profile leads to no spontaneous coupling, both algorithms will be holding *D* as a preferred action. The deviating player then must expect to play *C* with a strictly positive frequency while his opponent will keep on playing *D*, whereas under profile $(\varepsilon = 0, \varepsilon = 0)$ both algorithms end up playing *D* in the long run in the worst case scenario. Then, we leverage the results on extreme parameters to deduce that any Nash equilibrium must feature some spontaneous coupling.

We then perform extensive numerical simulations to investigate the behavior of algorithms for general profiles of exploration parameters. Results reveal that the dynamics are not different in essence than the ones uncovered by Banchio and Mantegazza (2023): spontaneous coupling might appear for moderate values of ε s. Using a simple clustering technique (namely K-means), we detect whether couples of parameters allow for spontaneous coupling, and with which probability it appears.

Under spontaneous coupling, algorithms enter cycles in which phases of cooperation alternate with phases of defection. Four regimes can be distinguished : *CC*, in which both algorithms prefer cooperation, *DD* when both prefer defection, *CD* (resp. *DC*) when *A* prefers *C* (resp. *D*) and *B* prefers *D* (resp. *C*). Increasing ε has several effects on an agent’s payoff. During phases in which this agent’s algorithm learns cooperation (typically *CC* phases), it has a positive effect on his payoff: since *C* is held as a preferred action, raising ε allows to explore more often and thus to play *D* with a higher frequency. Symmetrically, and for the same reason, it is detrimental during phases in which it learns defection. Moreover, increasing ε comes at the cost of potentially destroying the spontaneous coupling: in the extreme case in which one of the algorithms uses $\varepsilon = 1$, we prove that spontaneous coupling does not appear. As a consequence, no player has an incentive to set $\varepsilon = 1$. If a player, say *A*, did, it would cause both agents to hold *D* as a preferred action and *A* to play *C* half of the time. Finally, our simulations allow us to measure time spent in each of the four regimes, and to computationally find Nash equilibria of the designing game. They indicate that Nash equilibria are generally symmetric

and are located on a bell-shaped curve with respect to a parameter controlling for the value of cooperation.

The rest of the paper is organized as follows. Section 2 reviews the literature related to the present work, Section 3 formally introduces our model, Section 4 presents our analytical results regarding extreme exploration policies and Nash equilibria, Section 5 and 6 describe the simulations used to investigate more general policies and present their results, Section 7 concludes.

2 Related literature

The present article relates to a broad literature on Multi Agent Reinforcement Learning (MARL), which lies at the interface of computer science and game theory, and is mainly concerned with the interaction of several reinforcement learning algorithms. An introduction to this literature is given by Nowé et al, 2012 [29]. MARL presents the difficulty of having very few theoretical guarantees on the convergence of algorithms. Important contributions in the field have focused on designing algorithms that extend classical Q-learning, such as Tesauro, 2003 [32] with Hyper Q-learning and Hu, 2003 [19] with Nash Q-learning. Other authors have focused on building algorithms that maintain cooperation in prisoner’s dilemma like environment by adapting modern reinforcement learning techniques, such as Lere and Peysakhovich, 2017 [24] and Tampuu et al, 2017 [31]. Closer to our interest, Kianercy and Galstyan, 2012 [22] provide a full characterization of the rest points of a system composed of two Q-learning algorithms with Boltzmann exploration policy playing 2×2 games. Generally, it is well-known that some algorithms tend to learn cooperation when repeatedly playing a prisoner’s dilemma, see Banerjee and Sen, 2007 [6] for an example.

This work contributes more specifically to the literature on algorithmic collusion, which studies the interactions between Q-learning algorithms in economic situation. The possibility of spontaneous collusion by Q-learning algorithms has been receiving important attention in recent years. On the empirical side, Assad et al, 2020 [3] have provided evidence for algorithmic collusion on the German gasoline retail market, after algorithmic pricing methods became widely available in 2017. A similar phenomenon has been highlighted by Musolff et al, 2022 [28] using Amazon data. The policy implications and practical relevance of the topic are discussed in Calvano et al, 2019 [7]. On the theoretical side, the seminal contributions are those of Calvano et al, 2020 [8] and of Klein, 2021 [23]. Using extensive simulations, they show that Q-learning algorithms playing a repeated pricing game (in a Bertrand oligopoly in the first case, in a setting *à la* Maskin and Tirole, 1988 [26] in the second) learn to set supra-competitive prices in the long run. Calvano et al (2020) emphasize the *anatomy of collusion* constituted by punishment-reward schemes upon deviation, which is made possible by letting algorithms

condition their play on the previous action played by their opponent. In Klein (2021) on the other hand, long run behavior is characterized by asymmetric cycling prices rotating demand between players. Simulation-based extensions have followed. Calvano et al, 2021 [9] consider a setting with a Cournot duopoly with stochastic demand and show that a similar collusive behavior appears. Colliard et al (2022) [11] investigate the behavior of interacting Q-learning algorithms (*algorithmic market makers*) setting prices for a risky asset. Banchio and Skrzypacz, 2022 [5] consider Q learning algorithms repeatedly playing classical auction games, and interestingly report a difference between second price and first price auctions: in second price auctions, algorithms converge to the static equilibrium of the stage game, while in first price auction collusive behavior appears. Hettich, 2021 [18] runs simulations using a more advanced technology (namely deep Q-learning, see Mnih et al, 2015 [27] for a description of this deep reinforcement learning method) and obtains similar results than Calvano et al (2020) with a faster convergence to collusive behavior. Further extensions have been considered, typically by investigating the role of different market structures as in Sanchez-Cartas and Katsamakos, 2022 [30], or in Abada and Lambin, 2022 [1], which find similar results than Calvano et al (2020) on an economic environment replicating electricity markets. Further, Johnson et al, 2023 [20] study the effect of platform design on the behavior of Q-learning algorithms. They show that some platform designs that are effective for classical players turn out to be socially harmful in the presence of Q-learning algorithms, and point out a better adapted one.

Another branch of research, which the present work mostly builds on, have focused on understanding the mechanism responsible for collusion, which, as schematically explained in introduction, relies on the asynchronous nature of Q-learning’s updating. By simulating stateless Q-learning algorithms with ε -greedy policies, Asker et al, 2022 [2] provide evidence that collusive behavior is rooted in Q-learning’s asynchronous updating. They highlight that if algorithms have access to minimal information and are given minimal economic reasoning (specifically the demand being downward sloping), then collusion is substantially reduced. A similar phenomenon is observed by Banchio and Skrzypacz (2022) : letting Q-learning have access to the highest bid in previous period and letting them compute counterfactual scenarios when updating Q-values precludes collusive behavior. Finally, the contribution we build on most is the one of Banchio and Mantegazza (2023) [4], which characterizes limiting behavior of Q-learning algorithms playing a repeated prisoner’s dilemma using continuous time approximations. More precisely, they provide a theoretical bound on exploration level under which collusive behavior is possible¹. They highlight a phenomenon of *spontaneous coupling* between ε -greedy algorithms, and formally prove that letting algorithms synchronously update the Q-values prevents collusion.

The present article aims to fill a gap in the existing literature, which does not, in general,

¹A similarly flavored result was pointed out by Abada and Lambin (2022) using simulations

study settings with competition on the algorithms. A notable exception is Sanchez-Cartas and Katsamakas (2021), who compare Q-learning with Particle Swarm Optimization (PSO). PSO (Kennedy and Eberhart 1995 [21]) is a meta-heuristic method of optimization belonging to the class of evolutionary algorithms. Given a function to minimize (without knowing its gradient), PSO simulates the evolution of *candidate solutions* (seen as particles in a swarm). The particles move in the solution space depending on their own best known solution and the best known solution of the swarm, and oftentimes manage to collectively find optima. Their simulations indicate that, when PSO is competing with a stateless Q-learning algorithm, both set supracompetitive prices, however they do not consider the different technologies as being chosen in order to compete between each other. To the best of our knowledge, only Compte (2023) [12] integrates equilibrium considerations. In this paper, a variation of Q-learning integrating a possible bias towards cooperation is considered. Biases are chosen simultaneously by players before the algorithms start running. Simulations using a prisoners' dilemma indicate that Nash equilibria featuring positive bias towards cooperation exist and enhance collusive behavior. Finally, recent work by Dolgoplov (2024) [15] and Xu and Zhao (2024) [34] have provided further insight into the behavior of interacting Q-learning algorithms. Dolgoplov (2024) provides a full characterization of stochastically stable states of Q-learning algorithms repeatedly playing a prisoner's dilemma. He proves that under ε -greedy policies, the only stochastically stable outcome is for both algorithms to play defection, while depending on the payoffs and the learning rate, logit exploration allows for some cooperative behavior. In a similar way, Xu and Zhao (2024) prove that, for a wider class of games including prisoner's dilemma, Bertrand competition as well as first and second price auctions, in stochastically stable outcomes algorithms learn to play the strict Nash equilibrium of the game. They then give insight on why there is a difference between what stochastic stability allows and the empirical behavior of Q-learning algorithms using numerical simulations.

3 Setting and notations

3.1 Stage game

As in Banchio and Mantegazza (2023), the agents' algorithms repeatedly play a prisoner's dilemma which payoff matrix is presented in Table 1. We will denote this game $G_0(g)$, and $\tilde{\pi}_{X,Y}^P$ the payoff of player P under the profile (X, Y) in this game. $G_0(g)$ is a contribution game in which two players begin with an endowment of two monetary units and need to choose whether to invest it in a common pool. The common pool then grows by a factor g and is equally split between the two players. If a player does not invest their endowment in the pool, they get to keep it yet still receive half of the pool after it has grown. It is a special case of the prisoner's dilemma fully described by a unique parameter, g , whereas a prisoner's dilemma generally requires three. We mainly use this specification to compare our results with those of

Banchio and Mantegazza (2023) as well as to run extensive numerical simulations. However, our analytical results can be fully extended to general prisoner's dilemmas. The parameter g takes values in $[1, 2]$ and is interpreted as the value of cooperation. It has a two effects on the game. First, since $\tilde{\pi}_{CC}^A - \tilde{\pi}_{DD}^A = 2(g - 1)$, when g increases mutual defection becomes more socially detrimental. Conversely, when $g = 1$, $\tilde{\pi}_{CC}^A = \tilde{\pi}_{DD}^A$ so that there is no social cost to mutual defection. Second, as $\tilde{\pi}_{DC}^A - \tilde{\pi}_{CC}^A = 2 - g$ is decreasing with g , the incentive to deviate from mutual cooperation is decreasing with g and is eventually null when $g = 2$.

3.2 Q-learning

In our model, agents delegate their decision making to Q-learning algorithms. Q-learning is a simple reinforcement learning principle designed to find optimal solutions to optimization problems in a Markov environment. Formally, denote S a (finite) set of states, A a set of actions and $\pi(s, a)$ the (possibly stochastic) reward obtained in state s after taking action a . In each period, an action is taken, a reward is realized and the process moves to the next state with a probability $F(s_{t+1}|s_t, a_t)$. The objective is to learn the best policy, i.e. the one that maximizes $\mathbb{E}\left[\sum_{t=0}^{+\infty} \gamma^t \pi_t\right]$ with $\gamma \in (0, 1)$ an discount rate. Q-learning is an iterative method that allows to learn the best policy function without information or hypothesis about the transition function F . Classically, the Bellman value function in such a problem writes as follows:

$$\forall s \in S, V(s) = \mathbb{E}(\pi(s, a)) + \gamma \mathbb{E}(V(s')). \quad (1)$$

The Q-matrix assigns a value to each state-action pair, and is defined as

$$\forall (s, a) \in A \times S, Q(s, a) = \mathbb{E}[\pi|s, a] + \gamma \mathbb{E}[\max_{\{a' \in A\}} Q(s', a')|s, a], \quad (2)$$

and linked to the Bellman value function as follows

$$V(s) = \max_{a \in A} Q(s, a). \quad (3)$$

An agent who knows the Q-matrix exactly knows what action to take in each state, and thus knows the optimal policy. Q-learning estimates this matrix by an iterative procedure. The agent

		Player B	
		C	D
Player A	C	$2g, 2g$	$g, 2 + g$
	D	$2 + g, g$	$2, 2$

Table 1: Payoffs in the parameterized Prisoner's Dilemma

begins with an arbitrary Q_0 and updates any cell of the matrix she visits as follows:

$$Q_{t+1}(s, a) = (1 - \alpha)Q_t(s, a) + \alpha \left[\pi_t + \gamma \max_{a' \in A} Q_t(s', a) \right], \quad (4)$$

where α is referred to as the *learning rate* and controls how rapidly Q-values change when a reward is obtained. Note that when $\alpha = 0$ the Q-values stay constant, so that the agent does not learn, and when $\alpha = 1$ the Q-values immediately change to the actualized reward. Since our problem is stateless, the Q-matrix in this case is actually a vector, with one value per action. The update rule thus becomes, for all t , for all $a \in A$:

$$\begin{cases} Q_{t+1}(a) = (1 - \alpha)Q_t(a) + \alpha \left[\pi_t + \gamma \max_{a' \in A} Q_t(a) \right] & \text{if } a \text{ is played at } t \\ Q_{t+1}(a) = Q_t(a) & \text{otherwise.} \end{cases} \quad (5)$$

To decide which action to take given a matrix of Q-values, the agent relies on an *exploration policy*. The two most common exploration policies are *Boltzmann* and ε -*greedy*.²

Under Boltzmann exploration policy, the agent chooses an action a with probability

$$\mathbb{P}(a) = \frac{\exp(\lambda Q_t(a))}{\sum_{a' \in A} \exp(\lambda Q_t(a'))}, \quad (6)$$

where λ is a parameter controlling for the balance between exploration and exploitation. When $\lambda = 0$ the agent always chooses an action uniformly at random (i.e. always explores), whereas when $\lambda \rightarrow +\infty$ she always chooses the action with the highest Q-value (i.e. always exploits).

The policy we focus on is ε -greedy, under which the action chosen at time t is

$$a_t = \begin{cases} \arg \max_{a'} Q_t(a') & \text{with probability } 1 - \varepsilon \\ \sim \mathcal{U}(A) & \text{with probability } \varepsilon. \end{cases} \quad (7)$$

The main difference between ε -greedy and Boltzmann exploration policies is that the later is *smoother*: the other actions' Q-values being fixed, the probability with which an action a is chosen is increasing and continuously differentiable with respect to the Q-value of a . In the ε -greedy policy, the ε parameter plays a similar role than $\frac{1}{\lambda}$ for the Boltzmann policy: the higher ε the more frequently the agent explores. For $\varepsilon = 1$ the agent always chooses uniformly at random, conversely, when $\varepsilon = 0$ the agent *is greedy*: he always chooses the action with highest Q-value.

²We state the exploration policies in stateless environments, when there are several states the policy functions conditional on the state are the same.

3.3 Convergence of Q-learning algorithms

Convergence to the optimal Markov policy is guaranteed under conditions on the learning rates and on the exploration policy (Singh et al 2000):

Proposition (Singh et al). *Given a GLIE policy (Greedy in the Limit with Infinite Exploration), i.e. such that*

- *The exploration policy converges to the greedy one as t goes to ∞*
- *Every action-state pair is visited infinitely often,*

if the sequence of learning rates satisfy

1. $\sum_{t \in \mathbb{N}} \alpha_t = +\infty$
2. $\sum_{t \in \mathbb{N}} \alpha_t < +\infty,$

then $(Q_t)_{t \in \mathbb{N}}$ converges to the Q -matrix with probability 1.

In our setting, the above proposition cannot hold since we consider constant learning and exploration rates. This prevents the exploration policy to be GLIE. Though a similar and simpler result can be proven to hold in stateless environments.

Proposition 0. *Consider the simple maximization problem*

$$\max_{a \in \mathcal{A}} \pi_a \tag{8}$$

where \mathcal{A} is finite and for all a , $\pi_a \in \mathbb{R}$. Then, for any policy function ϕ such that any action is tried infinitely many times with probability 1, stateless Q-learning with exploration policy ϕ is such that, with probability 1:

$$\exists t^* \in \mathbb{N} \text{ s.t. } \forall t > t^*, \arg \max_{a \in \mathcal{A}} Q_t = \arg \max_{a \in \mathcal{A}} \pi_a. \tag{9}$$

This result relies on a simple argument: as the algorithm updates infinitely many times the Q-values associated to each action, it ends up realizing that some are better than others. When several Q-learning interact however, neither this result nor the previous one hold. As the algorithms react to each other's learning, their environment evolves, which might prevent them from settling for a preferred action. To illustrate this, consider the natural extension of the setting of Proposition 0 to two players. The payoff vector $(\pi_a)_{a \in \mathcal{A}}$ of the simple decision problem is replaced by a payoff matrix $(\pi_{a,a'})_{a,a' \in \mathcal{A}}$. Assume at t player A holds action a_1 as a preferred action and player B holds action $a = \arg \min_{a'} \pi(a', a_1)$ as a preferred action. If A keeps on holding it for long enough, B will eventually learn the action $a' = \arg \max_{a'} \pi(a', a_1)$. But since this will change B 's behavior, the payoff A will receive from now on will be different, so

that A can in return adapt its behavior. But since the behavior of A has changed, B can adapt as well and so on. The fact that each algorithm adapts to the other's behavior might thus prevent convergence to a pair of actions.

More formally, we can describe the process on Q-values as the iteration of a well-chosen operator. To construct it, for every profile $(X, Y) \in \{C, D\}^2$, we let $f_{X,Y}$ the function that associates to every \mathbb{Q} the vector of Q-value output by the update rule under profile $\{X, Y\}$. Thus, if at $t \in \mathbb{N}$ the vector of Q-values is $\mathbb{Q} \in \mathbb{R}^4$ and algorithms play profile $\{X, Y\}$, then the vector of Q-values at $t + 1$ will be $f_{X,Y}(\mathbb{Q})$. For any $\{X, Y\}$ in $\{C, D\}^2$, the function $f_{X,Y}$ is a well-defined bijection on \mathbb{R}^4 and we can denote $f_{X,Y}^{-1}$ its inverse function. We then define the following operator:

Definition 1. We call Q-operator, and denote \mathcal{Q} the mapping from $\Delta(\mathbb{R}^4)$ to $\Delta(\mathbb{R}^4)$ such that for all $\pi \in \Delta(\mathbb{R}^4)$ and for all $\mathbb{Q} \in \mathbb{R}^4$:

$$\mathcal{Q}(\pi)(\mathbb{Q}) = \sum_{\{X,Y\} \in \{C,D\}^2} \mathbb{P}(\{X, Y\} | \mathbb{Q}) \pi(f_{X,Y}^{-1}(\mathbb{Q})). \quad (10)$$

The Q-operator associates to a distribution π over the vector of Q-values an updated distribution. In particular, if the input distribution gives probability 1 to a specific vector of Q-values, then it outputs a distribution with non-0 probability for four vectors, one for each possible profile of actions. The Q-operator thus fully describes the possible evolutions of Q-values from one period to the other, and can be iterated to describe the whole process. We are particularly interested in whether this process converges to a limiting behavior, *i.e.* whether the sequence $\left(\mathcal{Q}^t(\pi_0)\right)_{t \in \mathbb{N}}$, converges or not, for an initial distribution π_0 . We leave this non-trivial question out of the scope of this paper and assume it does. Formally, we take the following assumption³:

Assumption 1. For all $\pi_0 \in \Delta(\mathbb{R}^4)$, $\mathcal{Q}^t(\pi_0)$, the sequence of distributions $\left(\mathcal{Q}^t(\pi_0)\right)_{t \in \mathbb{N}}$ weakly converges to some distribution $\bar{\pi}(\pi_0)$, where for $t \in \mathbb{N}$, $\mathcal{Q}^t(\pi_0)$ is recursively defined as $\mathcal{Q}^t(\pi_0) \equiv \mathcal{Q}(\mathcal{Q}^{t-1}(\pi_0))$.

Under this assumption, for any initial condition implemented in the algorithms, the distribution over the vector of Q-values reaches a limiting behavior. This assumption is crucial to define formally the payoff functions of the designer's game defined in Section 3.5.

3.4 Initial conditions

Even under our assumption, the limiting behavior of Q-values might depend on the initial conditions. As we focus on exploration parameters, we let initial conditions be chosen at random. More precisely, we focus on the following intervals. For $X \in \{C, D\}$, we denote

³Our simulations generally confirm this assumption.

$I_X^P = [\frac{\tilde{\pi}_{X,D}^P}{1-\gamma}, \frac{\tilde{\pi}_{X,C}^P}{1-\gamma}]$. Since for all g , $G_0(g)$ is symmetric, we let $I_X = I_X^A = I_X^B$. For $X \in \{C, D\}$, I_X is the interval in which the Q-value of action X should lie when X is played often enough *as a greedy action*. Its lower (resp. upper) bound is the value taken by $Q_P^X(t)$ if it were to be played infinitely many times as a greedy action while the opponent plays D (resp. C). We will say that the Q-value for an action X is *under (resp. over) evaluated* when it is lower (resp. larger) than the lower (resp. upper) bound of I_X . When X is played as a greedy action, three cases can be distinguished when it comes to its Q-value.

Proposition 1. *Consider a player P , $X \in \{C, D\}$ an action and $Q_P^X(t)$ the Q-value player P associates to action X at t . Assume $Q_P^X(t) > Q_P^{-X}(t)$ and P plays X at t . Then we can distinguish three cases:*

1. *If $Q_P^X(t)$ is under-evaluated, then $Q_P^X(t+1) > Q_P^X(t)$.*
2. *If $Q_P^X(t)$ is over-evaluated, then $Q_P^X(t+1) < Q_P^X(t)$.*
3. *If $Q_P^X(t) \in I_X$ then $Q_P^X(t+1) \geq Q_P^X(t) \iff -P$ plays C at t .*

Additionally, if $Q_P^X(t) \in I_X$, then $Q_P^X(t+1) \in I_X$.

The proof of this proposition is obtained by manipulating the update rule (Eq. 4). It allows us to characterize the behavior of Q-values, and to get the following proposition

Proposition 2. *Assume $\varepsilon_A, \varepsilon_B > 0$. Then with probability 1 there exists t such that:*

$$\forall P \in \{A, B\}, \forall X \in \{C, D\}, Q_P^X(t) \in [\frac{\tilde{\pi}_{X,D}^P}{1-\gamma}, \frac{\tilde{\pi}_{X,C}^P}{1-\gamma}] \equiv I_X. \quad (11)$$

This proposition guarantees that at some point, the process will end up in the Cartesian product $\mathbb{I} \equiv (I_C \times I_D)^2$. When exploration parameters are both different than 0, each action will be updated as a greedy action infinitely many times with probability 1. This will drive the Q-values inside \mathbb{I} if the initial conditions lie outside it. There are two caveats. First, the proposition does not hold when one of the players is greedy. Indeed, if a greedy player has both his Q-values underestimated initially, then the highest initial Q-value is updated in the first period, increases (Proposition 1) and the order is unchanged. By a trivial induction argument, the order of Q-values remains unchanged and the action with lowest initial Q-value is never updated. Second, even though some point of \mathbb{I} should be reached eventually, the probability with which each are reached might be different depending on initial conditions. Nevertheless, in order to simplify the discussion and to focus on the exploration parameters we will assume in the rest of the paper that the initial conditions are drawn uniformly and independently in \mathbb{I} .

3.5 Game on exploration parameters

Prior to letting algorithms play on their behalf, A and B need to simultaneously choose an exploration parameter $\varepsilon_A, \varepsilon_B \in [0, 1]$, implement it in their algorithm, let it play over a long enough period of time and collect the payoff obtained in the limit, which is well-defined under Assumption 1. This defines a *designing game* which we denote $G(g)$. Formally

$$G(g) = \langle P = \{A, B\}, S = \{[0, 1], [0, 1]\}, \Pi = \{\Pi^A, \Pi^B\} \rangle \quad (12)$$

where Π^A maps a profile of exploration policies $(\varepsilon_A, \varepsilon_B)$ to the average payoff obtained in the limit when A and B implement this profile in their algorithms.

Next we introduce useful notation to clarify the payoff function. For $P \in \{A, B\}, X \in \{C, D\}$, we denote $\omega_P^X = \{Q = (Q_A^C, Q_A^D, Q_B^C, Q_B^D) \in \mathbb{R}^4 \text{ s.t. } Q_P^X > Q_P^{-X}\}$ where $-X = C$ when $X = D$ and conversely. Further, for $X, Y \in \{C, D\}$ we denote $\omega_{X,Y} = \omega_A^X \cap \omega_B^Y$. Geometrically, ω_P^X corresponds to the half \mathbb{R}^4 space in which algorithm P holds action X as a preferred action. Similarly, $\omega_{X,Y}$ corresponds to the quarter of space in which algorithms A and B respectively hold actions X and Y as preferred actions. As the process goes, $(Q_t)_{t \in \mathbb{N}}$ moves across \mathbb{R}^4 and changes region. Under convergence to a stationary distribution, in the limit, the process spends on average some time in each region. For all $X, Y \in \{C, D\}$, we let $\tau_{X,Y}^g(\varepsilon_A, \varepsilon_B) \in [0, 1]$ the average fraction of time spent in region $\omega_{X,Y}$ in the long run when repeatedly playing $G_0(g)$. More formally, if at t the system has reached its limit behavior:

$$\tau_{X,Y}^g(\varepsilon_A, \varepsilon_B) = \mathbb{P}(Q_t \in \omega_{X,Y}) \quad (13)$$

The expected payoff to players at t only depends on the region Q_t is in. Indeed, being in region $\omega_{X,Y}$ guarantees that player A will play action X with probability $1 - \frac{\varepsilon_A}{2}$ and action $-X$ with probability $\frac{\varepsilon_A}{2}$, while B will play action Y with probability $1 - \frac{\varepsilon_B}{2}$ and action $-Y$ with probability $\frac{\varepsilon_B}{2}$.⁴ Thus, conditional on staying in region $\omega_{X,Y}$ the payoff to both players follows a well-defined distribution. Their expectations are interpreted as the average payoffs players collect when their Q-values stay in $\omega_{X,Y}$ for a long time, which enables us to give an expression to the payoff function in $G(g)$. For all X, Y , we let $\pi_P^{X,Y}(\varepsilon_A, \varepsilon_B)$ be the average payoff to player P in zone $\omega_{X,Y}$, and get :

$$\begin{cases} \pi_A^{C,C} = (1 - \frac{\varepsilon_A}{2})(1 - \frac{\varepsilon_B}{2}).2g + (1 - \frac{\varepsilon_A}{2})\frac{\varepsilon_B}{2}.g + \frac{\varepsilon_A}{2}(1 - \frac{\varepsilon_B}{2}).(2 + g) + \frac{\varepsilon_A}{2}\frac{\varepsilon_B}{2}.(2) \\ \pi_A^{C,D} = (1 - \frac{\varepsilon_A}{2})(1 - \frac{\varepsilon_B}{2}).g + (1 - \frac{\varepsilon_A}{2})\frac{\varepsilon_B}{2}.2g + \frac{\varepsilon_A}{2}(1 - \frac{\varepsilon_B}{2}).2 + \frac{\varepsilon_A}{2}\frac{\varepsilon_B}{2}.(2 + g) \\ \pi_A^{D,C} = (1 - \frac{\varepsilon_A}{2})(1 - \frac{\varepsilon_B}{2}).(2 + g) + (1 - \frac{\varepsilon_A}{2})\frac{\varepsilon_B}{2}.2 + \frac{\varepsilon_A}{2}(1 - \frac{\varepsilon_B}{2}).2g + \frac{\varepsilon_A}{2}\frac{\varepsilon_B}{2}.g \\ \pi_A^{D,D} = (1 - \frac{\varepsilon_A}{2})(1 - \frac{\varepsilon_B}{2}).2 + (1 - \frac{\varepsilon_A}{2})\frac{\varepsilon_B}{2}.(2 + g) + \frac{\varepsilon_A}{2}(1 - \frac{\varepsilon_B}{2}).g + \frac{\varepsilon_A}{2}\frac{\varepsilon_B}{2}.2g \end{cases} \quad (14)$$

⁴Indeed, for player A (resp. B) action $-X$ (resp. $-Y$) is only played when A (resp. B) explores, which happens with probability $\frac{\varepsilon_A}{2}$ (resp. $\frac{\varepsilon_B}{2}$) and the uniform exploration chooses action $-X$ (resp. $-Y$), which happens with probability $\frac{1}{2}$.

The payoff function of A in $G(g)$ then writes

$$\Pi^A(\varepsilon_A, \varepsilon_B) = \sum_{(X,Y) \in \{C,D\}^2} \tau_{X,Y}^g(\varepsilon_A, \varepsilon_B) \pi_{X,Y}^A(\varepsilon_A, \varepsilon_B). \quad (15)$$

The corresponding quantities for B are deduced by symmetry. We interpreted this quantity as follows: when players choose ε_A and ε_B , for each couple of actions (X, Y) their algorithms spend on average a fraction $\tau_{X,Y}^g(\varepsilon_A, \varepsilon_B)$ of their time in $\omega_{X,Y}$. On average, each period spent in $\omega_{X,Y}$ gives player A a payoff of $\pi_{X,Y}^A(\varepsilon_A, \varepsilon_B)$. We are mostly interested in the *Nash equilibria* of this game, as well as the profiles of exploration levels $(\varepsilon_A, \varepsilon_B)$ that maximize the joint payoff. Formally:

Definition 2. Profile $(\varepsilon_A, \varepsilon_B)$ is called **Pareto optimal** if

$$(\varepsilon_A, \varepsilon_B) \in \arg \max_{(\varepsilon'_A, \varepsilon'_B) \in [0,1]^2} \left(\Pi^A(\varepsilon'_A, \varepsilon'_B) + \Pi^B(\varepsilon'_A, \varepsilon'_B) \right). \quad (16)$$

3.6 Former results

3.6.1 Continuous time approximation

In order to study the complex behavior of the two interacting Q-learning algorithms, a useful object to rely on is its *continuous time approximation*. The continuous time approximation provides a representation of this process as a dynamical system, both deterministic and continuous. It consists in a set of differential equations describing a *flow* which enables to study the motion of Q-values in the four dimensional space as deterministic (continuous) trajectories rather than stochastic (discrete) ones. Banchio and Mantegazza (2023) prove that a continuous time approximation is well defined for a wide class of reinforcement learning procedures, among which Q-learning with ε -greedy exploration policy. In our problem, a continuous time approximation is defined on the interior of each $\omega_{X,Y}$. The proof of existence and the formal construction of continuous time approximations are provided by Banchio and Mantegazza (2023) (Sec. 2.2.), here we only give an intuition of what the continuous time approximation is.

In the original system, time is discrete and updates are random. Given a vector of Q-values, the vector of Q-values can take four different values next period, depending on the profile of actions played by the algorithms. When $\mathbb{Q}_t = \mathbb{Q} \in \mathbb{R}^4$, there is thus an *expected* vector of Q-values for period $t + 1$. This expected vector is the value \mathbb{Q}_{t+1} would take if, instead of being updated randomly, \mathbb{Q}_t was updated deterministically and "on average". We approximate the motion of the discrete and stochastic system by trajectories following the expected vector of Q-values. This corresponds to the following procedure. Assume that instead of updating the system once every time period, we were to generate two possible updates and to give each of

these half the weight a normal update (in the original system) has. Then, by the end of the period, this new system would be updated as an average of the two generated updates. Now assume that the number of updates generated this way increases, the size of time intervals and the weight of each update goes to 0, and instead of taking the value of the expected vector of Q-values, Q_t moves slightly *in the direction* of the expected vector. The continuous time approximation describes this as a *flow*: it is a system of differential equations describing, for each position of Q the derivative with respect to time of Q_t .

In order to distinguish the stochastic process generated by the actual Q-values (in discrete time) from its continuous time approximation, we will denote the latter

$$(\tilde{Q}_t)_{t \in \mathbb{R}} = \left(\left(\tilde{Q}_A^C(t), \tilde{Q}_A^D(t), \tilde{Q}_B^C(t), \tilde{Q}_B^D(t) \right) \right)_{t \in \mathbb{R}} \quad (17)$$

as opposed to $(Q_t)_{t \in \mathbb{N}}$. By applying Theorem 1 in Banchio and Mantegazza (2023, Sec. 2.2), in region $\omega_{X,Y}$ the dynamics of the continuous time approximation for the Q-values of player A can be written as:

$$\begin{cases} \dot{\tilde{Q}}_A^X(t) = \alpha \left(1 - \frac{\varepsilon_A}{2}\right) \left[\hat{\pi}_{X,Y} - (1 - \gamma) \tilde{Q}_A^X(t) \right] \\ \dot{\tilde{Q}}_A^{-X}(t) = \alpha \frac{\varepsilon_A}{2} \left[\hat{\pi}_{-X,Y} + \gamma \tilde{Q}_A^X(t) - \tilde{Q}_A^{-X}(t) \right], \end{cases} \quad (18)$$

where $\hat{\pi}_{X,Y}$ is the average payoff to player A when she plays action X while in region $\omega_{X,Y} \cup \omega_{-X,Y}$, i.e.

$$\hat{\pi}_{X,Y} = \left(1 - \frac{\varepsilon_B}{2}\right) \tilde{\pi}_{X,Y} + \frac{\varepsilon_B}{2} \tilde{\pi}_{X,-Y}. \quad (19)$$

3.6.2 Filippov solutions

The continuous time approximation of our system is not defined at the border of each $\omega_{X,Y}$ and is thus piece-wise discontinuous. This is due to the probability of selecting a certain action brutally changing when the order of Q-values is reversed. A well-adapted concept to such cases has been defined and studied by Filippov (1960) [16]. *Filippov solutions* appear when the flow of a dynamical system has opposite directions along a border. Consider for example the following simple system of differential equations, denoted (S), such that for $(x, y) \in \mathbb{R} \times \mathbb{R}_+^*$

$$(S) : \begin{cases} \dot{x}(t) = x(t) - 10 \\ \dot{y}(t) = \exp(y(t)) \end{cases} \quad (20)$$

and for $(x, y) \in \mathbb{R} \times \mathbb{R}_-^*$

$$(S) : \begin{cases} \dot{x}(t) = x(t) - 10 \\ \dot{y}(t) = -\exp(y(t)) \end{cases} \quad (21)$$

This dynamical system is piece-wise continuous with a discontinuity on the y -axis. (S) clearly doesn't have a steady state in the classical sense. However, on both sides of the discontinuity, its flow has opposite directions, which allows to define a Filippov solution. To find a Filippov solution, we proceed in two steps. First, we look for coefficients τ_1 and τ_2 , with $\tau_1 + \tau_2 = 1$ such that

$$\left(\tau_1 \begin{bmatrix} x - 10 \\ \exp(y) \end{bmatrix} + \tau_2 \begin{bmatrix} x - 10 \\ -\exp(y) \end{bmatrix} \right) \cdot \vec{N} = 0, \text{ where } \vec{N} = \begin{bmatrix} 0 \\ 1 \end{bmatrix} \quad (22)$$

This step constructs a new flow as a linear combination of flows on both sides of the discontinuity, such that its normal component to the discontinuity is null. It is crucial in defining the Filippov solution, and the new flow is referred to as a *sliding vector*. It has the following interpretation. By spending a fraction of time τ_1 in \mathbb{R}_+^* and a fraction of time τ_2 in \mathbb{R}_-^* , the system stays, on average, on the discontinuity. The newly defined flow thus corresponds to the motion of the system *sliding* along the discontinuity. In the case of (S) we easily solve for τ_1 and τ_2 and find $\tau_1 = \tau_2 = \frac{1}{2}$, thus giving us $(x - 10, 0)$ as a sliding vector. As the system slides on the y -axis, it may reach a point at which it doesn't move anymore, which we call a *pseudo steady-state*. This amounts to finding a point that sets the sliding vector to 0. In the case of (S), $(x = 10, y = 0)$ is a pseudo-steady state. Thus, at the pseudo-steady state of (S), half of the time is spent in \mathbb{R}_+^* , half of the time is spent in \mathbb{R}_-^* , and the system stays *on average* at the position $(10, 0)$.

3.6.3 Spontaneous coupling with symmetric parameters

Under the assumption of symmetry in the initial condition (i.e. $\forall X \in \{C, D\}, \tilde{Q}_A^X(0) = \tilde{Q}_B^X(0)$), the continuous time approximations remains in $\omega_{CC} \cup \omega_{DD}$, allowing Banchio and Mantegazza (2023) to prove the following result in the case $\varepsilon_B = \varepsilon_A = \varepsilon$:

Proposition (Banchio and Mantegazza (2023)). *Let $\underline{\varepsilon}(g) = 1 - \sqrt{\frac{2-g}{g}}$. If $\varepsilon > \underline{\varepsilon}(g)$ then all initial conditions lead to $Q_D^{eq} = \left(\frac{2\varepsilon+2g-\varepsilon g}{2} + \frac{\gamma(4+\varepsilon g)}{2(1-\gamma)}, \frac{4+\varepsilon g}{2(1-\gamma)} \right) \in \omega_{DD}$. If $\varepsilon \leq \underline{\varepsilon}(g)$ a pseudo steady-state Q_C^{eq} exists and lies in ω_{CC} .*

The pseudo steady-state in this proposition captures the behavior of the Q-values alternating between phases in ω_{CC} and ω_{DD} . In ω_{CC} phases, Q-values for both C and D increase, however Q-values for D tend to increase faster causing the system to eventually go back to ω_{DD} . In ω_{DD} phases, Q-values for both C and D decrease, leaving a possibility to transition from ω_{DD} back to ω_{CC} . This alternating behavior can only appear when the exploration policies are low enough. Indeed, the Q-values for C should not decrease too fast when the system is in ω_{DD} , otherwise it will not switch to CC again. For this not to happen, the frequency of exploration should be low enough so as for C not to be played (and thus updated) too often during ω_{DD} phases. An increase in ε leads to an increase in the frequency with which the Q-values for D are updated and thus the speed with which they increase. As a consequence, a higher ε leads to less

time spent in ω_{CC} phases. Following the terminology introduced by Banchio and Mantegazza (2023), we will refer to this phenomenon as *spontaneous coupling*.

3.7 Spontaneous coupling in the general case

In the general case, i.e. when exploration parameters are different, the continuous time approximation can be studied region by region, allowing to get the following result

Proposition 3. $\forall (\varepsilon_A, \varepsilon_B, g) \in [0, 1] \times [0, 1] \times [1, 2]$, there exists a steady state \tilde{Q}_{DD}^{eq} of the continuous time approximation that lies in ω_{DD} . No other steady-state exists.

The proof of this result is in two steps. First, we show that there is indeed a point in ω_{DD} that sets the flow of the continuous time approximation to 0. Second, for any other region $\omega_{X,Y}$, if we assume that there is a steady-state in $\omega_{X,Y}$, then it should lie in ω_{DD} . Thus in any other region, the system is pushed towards ω_{DD} . As an example, consider what happens when both algorithms hold C as a preferred action, which in terms of continuous time approximation corresponds to looking at the flow at $Q \in \omega_{C,C}$. In such part of the space, even though D might be updated rarely (especially if ε is low), when it is, it increases more frequently than it decreases. This is due to the fact that C is played more often by the opponent's algorithm than D , and thus the Q-value of D will increase on average. In continuous time approximation terms, this translates into a positive value for D 's Q-value's derivative. As a steady state in ω_{DD} always exists, we should expect a non-spontaneous coupling outcome to be possible for all values of parameters.

Naturally, we would like to extend the reasoning of Banchio and Mantegazza (2023) to the general case and look for Filippov solutions of the continuous time approximation. This however is not possible as the hypothesis of symmetry in the initial conditions no longer guarantees the system to stay in $\omega_{CC} \cup \omega_{DD}$. This prevents Filippov solutions to be defined as it would require defining a sliding vector on a set of co-dimension 2, which, as well known in the specialized literature (see Dieci et al (2011, 2013) [14, 13]) is not generally possible. We thus cannot give a definition of spontaneous coupling as the existence of a Filippov pseudo-equilibrium of the continuous time approximation. To circumvent this difficulty, we give the following definition to spontaneous coupling:

Definition 3. Let $(\varepsilon_A, \varepsilon_B, g) \in [0, 1] \times [0, 1] \times [1, 2]$. We say $(\varepsilon_A, \varepsilon_B, g)$ *allows for spontaneous coupling* iff there exists $Q_0 \in \mathbb{R}^4$ such that:

$$\forall S \subset \mathbb{R}^4 \text{ s.t. } , \mathbb{P}(\exists t \in \mathbb{N}, Q_t \in S | Q_0) = 1, \exists \tilde{Q}_0 \in S \text{ s.t. } \neg \left(\lim_{+\infty} \tilde{Q}_t(\varepsilon_A, \varepsilon_B, g, \tilde{Q}_0) = \tilde{Q}_{DD}^{eq} \right). \quad (23)$$

Further, we define the **basin of attraction** of spontaneous coupling as

$$\mathcal{B}(\varepsilon_A, \varepsilon_B, g) = \{\tilde{\mathbb{Q}}_0 \in \mathbb{I} \text{ s.t. } \lim_{+\infty} \tilde{Q}_t(\varepsilon_A, \varepsilon_B, g; \tilde{\mathbb{Q}}_0) \neq \tilde{\mathbb{Q}}_{DD}^{eq}\} \quad (24)$$

and its size as

$$\mathcal{S}(\varepsilon_A, \varepsilon_B, g) = \lambda(\mathcal{B}(\varepsilon_A, \varepsilon_B, g)) \quad (25)$$

where $\lambda(\cdot)$ is the Lebesgue measure on \mathbb{R}^4 .

We use both the (discrete) dynamics of Q-learning algorithms and their continuous counterpart to define spontaneous coupling. The continuous time approximation describes an averaged behavior of the algorithms. However, when $\varepsilon_A = 0$ or $\varepsilon_B = 0$ the actual dynamics of Q-learning algorithms are affected by rare events, causing the continuous time approximation to poorly describe them. In our definition, we thus require that in the long run, the "averaged version" of the system features some time spent in any other region than ω_{DD} and the actual system does not end up in ω_{DD} . More precisely, we require that, whenever the actual stochastic discrete process with initial condition \mathbb{Q}_0 is guaranteed to end up in a set S at some point in time, the continuous time approximation starting at some point in S should not end up in the ω_{DD} steady-state in the limit. If such an S exists, we know that the stochastic process will end up in S at some point, and then be attracted "on average" by the ω_{DD} steady-state.

4 Behavior of the system for extreme parameters

As a first step, we characterize the behavior of the algorithms when one of the players uses an extreme exploration parameter, that is when for some $P \in \{A, B\}$, $\varepsilon_P = 0$ or $\varepsilon_P = 1$. In these cases, the system behaves in a simpler way, allowing us to get analytical results on the possibility of spontaneous coupling.

Proposition 4. *For any $g \in [0, 1]$, if $\varepsilon_A = 1$ or $\varepsilon_B = 1$, $(\varepsilon_A, \varepsilon_B, g)$ does not allow for spontaneous coupling.*

The intuition for this result is the following. Whenever one player, say A , adopts $\varepsilon_A = 1$, her behavior becomes constant over time: she always fully randomizes between the two actions. As a consequence, the environment for B 's algorithm becomes stationary, allowing it to learn to defect in the long run. This remains true for any value of ε_B , especially for $\varepsilon_B = 1$, in line with Banchio and Mantegazza (2023)'s result.

We get a similar result in the case $\varepsilon_A = 0$ and $\varepsilon_B > 0$:

Proposition 5. *For any $g \in [0, 1]$, if $\varepsilon_A = 0$ and $\varepsilon_B > 0$, $(\varepsilon_A, \varepsilon_B, g)$ does not allow for spontaneous coupling.*

In this case, one player is fully greedy while the other uses a non-zero exploration parameter. This result is counter-intuitive given the role of exploration levels in the symmetric setting. In the symmetric case, spontaneous coupling can appear for any profile $(\varepsilon, \varepsilon)$ with $\varepsilon < \underline{\varepsilon}(g)$. One could thus expect spontaneous coupling to appear for all asymmetric profiles $(\varepsilon_A, \varepsilon_B)$ with $\varepsilon_A, \varepsilon_B < \underline{\varepsilon}(g)$. This proposition contradicts this intuition and highlights the role of asymmetry in preventing spontaneous coupling, at least in the extreme case in which $\varepsilon_P = 0$ for some $P \in \{A, B\}$.

The proof relies on the following arguments. Say $\varepsilon_A = 0$ and $\varepsilon_B > 0$: player A is fully greedy, and player B is not. Then for player A , at each period, only the action with highest Q-value is played, and thus updated. As a consequence, Proposition 1 always applies, and the updated Q-value increases if B plays C and decreases if B plays D . Also, the Q-value for action $X \in \{C, D\}$ cannot exit I_X . Note that I_C and I_D overlap but are not included in one another. As a consequence, if ever the Q-value for C gets below $\frac{2}{1-\gamma}$ (the lower bound I_D), then it will remain below the Q-value for D forever on. Furthermore the minimal Q-value (which is not updated) is a decreasing sequence. Indeed, when there is no change in the order of Q-values it remains unchanged, and when there is a change in the order it can only be because the maximal Q-value decreased and got below the minimal one. As long as both Q-values remain in the intersections of their I_C and I_D , they will sequentially undercut each other with probability 1, causing the minimal Q-value to get closer and closer to the bound of I_D . But then, at some point and with probability 1, the Q-value for C will decrease by a large enough amount when it is close enough to this lower bound. When this happens, the Q-value for C exits I_D and the latter will remain above the first one forever on. Then, the behavior of A becomes stationary: she only plays D , causing B to adapt and learn D in the long run as well. This proof crucially relies on the fact that some events happen almost surely in the long run. As the minimal Q-value decreases in a non-reversible way, it is inevitably driven towards outside I_D in the long run. Thus, the behavior of the system highlighted by this proposition is specific to the case where $\varepsilon_B > 0$ and does not hold when $\varepsilon = 0$. Note as well that this result can be easily generalized to broader classes of policy functions (see the Appendix) or to other 2×2 games.

These two results give nuance to the interpretation we gave to the effect of exploration on spontaneous coupling. We stated that too high exploration levels would break spontaneous coupling as if it appeared when, and only when, the "total level" of exploration is low enough. Decreasing the exploration level of one agent actually does not necessarily counterbalance the high exploration level of another. Specifically, no matter how small ε_B is, when ε_A is equal to 1 no spontaneous coupling is reached at all, and similarly when $\varepsilon_A = 0$.

Finally, we partially characterize the behavior of the system when when both algorithms are greedy ($\varepsilon_A = \varepsilon_B = 0$).

Proposition 6. *For any g , $(0, 0, g)$ allows for spontaneous coupling. More specifically for any initial condition in \mathbb{I} , there exists $t^* \in \mathbb{N}$ such that for all $t > t^*$, $\mathbb{Q}(t) \in \omega_{CC}$ or $t^* \in \mathbb{N}$ such that for all $t > t^*$, $\mathbb{Q}(t) \in \omega_{DD}$. Furthermore, $\tau_{CC}^g(0, 0) \geq 4\left(1 - \frac{1}{g}\right)^4 \in [0, \frac{1}{4}]$.*

In this case, the system is completely deterministic and fully determined by the initial condition. Proposition 1 applies for both algorithms, so that when the system gets in ω_{CC} it remains in ω_{CC} , which allow us to get the lower bound on $\tau_{CC}^g(0, 0)$. The proof then proceeds to show that either in the long run the system gets stuck in ω_{CC} or it gets stuck in ω_{DD} by a similar mechanism than uncovered in the previous proposition. However, we are not able to give exact probability for the two events. There is indeed the possibility that, even though the system began in ω_{DD} it transitions to ω_{CC} and remains there for ever on. For this to happen, the system should be in ω_{DD} the period right before. Otherwise, if it is in ω_{CD} (or equivalently ω_{DC}), player's B Q-value for D increases and the system can thus either stay in ω_{DC} or go to ω_{DD} . For it to transition to ω_{CC} , Q-values for D for both players should undercut that of C at the same period. Although unlikely to happen, this event cannot be ruled out.

5 General properties of $G(g)$

The previous results concerning the possibility of spontaneous coupling for extreme values of parameters allow us to draw conclusions concerning the game $G(g)$.

Proposition 7. *For all $g \in [1, 2]$, $(\varepsilon_A = 0, \varepsilon_B = 0)$ is a Nash equilibrium of $G(g)$. It is strict whenever $g > 1$.*

Proof. Assume $\varepsilon_B = 0$, then if A chooses $\varepsilon_A > 0$, $\tau_{DD}^g(\varepsilon_A, \varepsilon_B) = 1$ (Proposition 4). Then A receives payoff:

$$\Pi^A(\varepsilon_A, 0) = 2\left(1 - \frac{\varepsilon_A}{2}\right) + g\frac{\varepsilon_A}{2} \leq 2. \quad (26)$$

However, if A uses $\varepsilon_A = 0$ then she gets payoff

$$\Pi^A(0, 0) = 2\tau_{DD}^g(0, 0) + 2g\tau_{CC}^g(0, 0) \geq 2. \quad (27)$$

We deduce the result by symmetry of the game. □

Loosely speaking, if player A were to know there will be no spontaneous coupling, she would not play $\varepsilon > 0$ playing. In this case both algorithms will learn D , thus it is clear that any exploration is only counterproductive: it implies playing C with positive probability. Since when B chooses $\varepsilon_B = 0$ spontaneous coupling will not appear whenever $\varepsilon_A > 0$, the best response for A is to choose $\varepsilon_A = 0$ as well.

This result makes clear that exploration is harmful when there is no spontaneous coupling. We use the same idea to prove the following proposition:

Proposition 8. *For all $g \in]1, 2[$, $\varepsilon = 1$ is a dominated strategy in $G(g)$.*

Playing $\varepsilon = 1$ cannot be optimal, and is actually the worst possible choice. We formally prove this result by showing $\varepsilon = 0$ dominates $\varepsilon = 1$.

Proof. Let $\varepsilon_A \in]0, 1[$. If $\varepsilon_B = 1$, then we know from Proposition 3 that $(\varepsilon_A, \varepsilon_B, g)$ does not allow for spontaneous coupling and thus $\tau_{DD}^g = 1$. Thus player B will receive payoff:

$$\Pi^B(\varepsilon_A, 1) = \left(1 - \frac{\varepsilon_A}{2}\right) \frac{g+2}{2} + \frac{\varepsilon_A}{2} \frac{2g+2+g}{2} \quad (28)$$

whereas by playing $\varepsilon_B = 0$ still $(\varepsilon_A, \varepsilon_B, g)$ does not allow for spontaneous coupling and he would get payoff:

$$\Pi^B(\varepsilon_A, 0) = \left(1 - \frac{\varepsilon_A}{2}\right) \cdot 2 + \frac{\varepsilon_A}{2} (2+g), \quad (29)$$

which is clearly higher than the latter. Now assume $\varepsilon_A = 0$, then we already know from Proposition 6 that $(0, 0)$ is a strict Nash equilibrium in $G(g)$ which completes the proof. \square

When a player chooses to set his own exploration to 1, he makes a non optimal choice in two ways. First, he guarantees that no spontaneous coupling will happen (Proposition 3). Second, he puts himself in the worst situation *conditional on* no spontaneous coupling being reached: he chooses the highest exploration level which will make him play C half of the time.

The intuition used for those two results generalize to get the following proposition:

Proposition 9. *For any $g \in]1, 2[$, if $(\varepsilon_A, \varepsilon_B)$ is a Nash equilibrium of $G(g)$ then $(\varepsilon_A, \varepsilon_B, g)$ allows for spontaneous coupling. More specifically, $\tau_{CC}^g(\varepsilon_A, \varepsilon_B) > 0$ or $\left(\tau_{CD}^g(\varepsilon_A, \varepsilon_B) > 0 \text{ and } \tau_{DC}^g(\varepsilon_A, \varepsilon_B) > 0\right)$*

The proof of this result is by contradiction. Let $(\varepsilon_A, \varepsilon_B)$ a Nash equilibrium with no spontaneous coupling allowed. Since no spontaneous coupling is allowed, $(\varepsilon_A, \varepsilon_B)$ cannot be $(0, 0)$ (Proposition 5), thus either $\varepsilon_A \neq 0$ or $\varepsilon_B \neq 0$. Assume without loss of generality that ε_B is not equal to 0. Since it is a Nash equilibrium, the exploration parameter that maximizes A 's payoff given ε_B is such that $\lambda(\mathcal{B}(\varepsilon_A, \varepsilon_B)) = 0$. But then, the exploration parameter that maximizes A 's payoff and checks that condition is no other than $\varepsilon_A = 0$. Indeed, if no spontaneous coupling appears, it is always better to play the lowest exploration policy possible, i.e. 0. Then, the Nash equilibrium is of the form $(0, \varepsilon_B)$, but since $(0, 0)$ is a strict Nash equilibrium, we get a contradiction. Further, the second part of the proposition guarantees that, in a Nash equilibrium, a (spontaneous coupling) outcome should not be too unfavorable to a player. In such

a case, he would be able to easily break the unfavorable spontaneous coupling and secure the highest payoff among outcomes without spontaneous coupling.

This gives an answer to our initial question: spontaneous coupling *does not disappear in equilibrium*. This result can be extended to a more general case, in which initial conditions and other parameters are chosen strategically, and in which a wider class of exploration policies is available for choice, as long as it contains the greedy policy. This result is important as it enables to focus on cases in which spontaneous coupling is indeed reached and guarantees that, with two players, spontaneous coupling will not be destroyed by the competition on algorithms' design. Any equilibrium on which algorithm designers might coordinate by simultaneously choosing their algorithmic technology in a class of exploration policies will leave space for spontaneous coupling and thus for cooperative behavior between the two algorithms. This result crucially relies on the fact that trying to "over-exploit" the other's cooperative behavior by raising one's own level of exploration is punished by the system not allowing coupling, causing the exploiter to incur losses due to his exploration rate. This is due to each algorithm individually having an important impact on the system's behavior. It might thus be the case that, if we had a similar game with infinitely many algorithms each of which have a negligible effect on the dynamics of the whole, the conclusion would be the opposite. As one algorithm's level of exploration has no effect whatsoever on other algorithms' tendencies to cooperate, the optimal individual choice would always be to choose $\varepsilon = 1$, leading all players to choose it in equilibrium.

6 General case

In order to further investigate the interaction between our Q-learning algorithms, we run extensive simulations. Our primary goal is to understand how exploration policies affect the existence and the properties of spontaneous coupling.

6.1 Methodology

We begin by generating the stage game $G_0(g)$ for a chosen parameter g , then simulate the algorithms between $2 \cdot 10^4$ and 10^5 periods (depending on the computational intensity of the simulations considered). We fix $\gamma = 0.95$ and $\alpha = 0.1$, and vary g, ε_A and ε_B . We divide the set of possible parameters into 20^3 triplets, where possible values for one parameter are equally spaced on the corresponding interval. For each triplet $(g, \varepsilon_A, \varepsilon_B)$ the process is simulated between 50 and 100 times, and metrics we get from the simulations are then averaged. We extract relevant quantities from these simulations, namely the Q-values and the actions played upon reaching convergence. In practice, we take the last 100 or 1000 periods of every run and assume it has reached convergence by that moment.

We measure the frequency with which actions are played in the long run and more importantly

the frequency with which they are learned in the long run. This aggregates two things: first, the time spent in each portion of the space in a pseudo-equilibrium (when it is reached) and the probability with which such pseudo-equilibrium is reached. We take this measure as an estimation of $\tau_{X,Y}$, for $\{X, Y\} \in \{C, D\}^2$, the average time spent in each region in the long run.

6.2 Symmetric profiles

We begin by looking at the symmetric case, i.e. choose $\varepsilon_A = \varepsilon_B$ (the setting of Banchio and Mantegazza (2023)) to see the difference between existence of pseudo-equilibrium and actually reaching it. In Figure 1, we show the difference between the actual time spent in ω_{CC} and the theoretical time spent inside once the equilibrium is reached (as given by Proposition 3.6.3. On the heatmap of the left panel, the cells represent a triplet $(g, \varepsilon, \varepsilon)$ and their colors depend on the frequency with which action C is learned. Dark cells thus correspond to triplets for which cooperation is seldom learned in the long run, while light ones are those for which cooperation is often held as a best action. The white curve is the theoretical boundary obtained by Banchio and Mantegazza (2023) (Proposition 3.6.3), above which spontaneous coupling is no longer possible. Indeed, passed $\underline{\varepsilon}(g)$, agents do not learn to cooperate⁵. However, inside the region for which a pseudo steady-state is theoretically possible, we observe that it is not necessarily reached. In particular, for low values of g , it seems that D is never learned. For intermediate values, when ε is low, D is rarely learned. When $\varepsilon = 0$, the frequency with which D is learned is high, and decreases with g , which is consistent with Proposition 4. For low exploration policy and for intermediate values of g , C is rarely learned. We explain this by the fact that, when ε is very low, the system behaves deterministically for long periods of time.

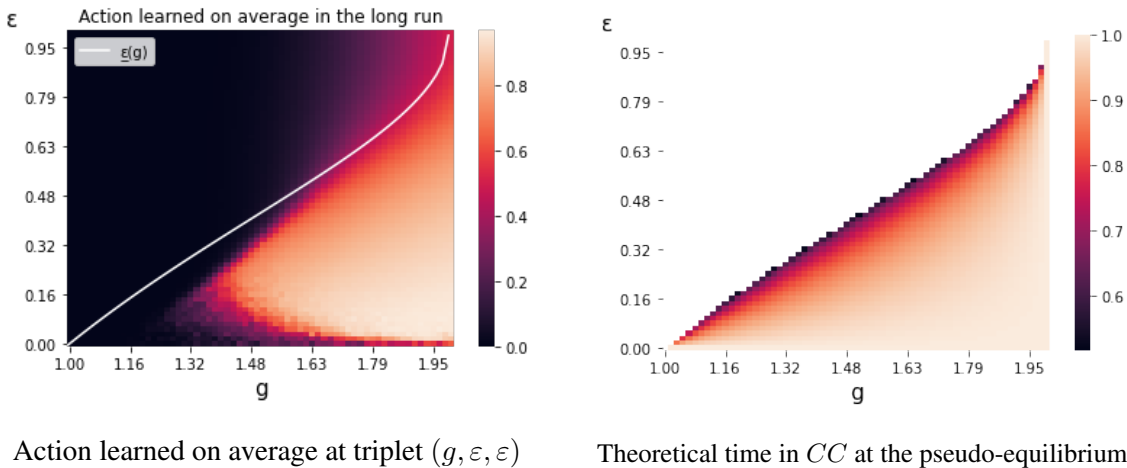


Figure 1: Time spent in ω_{CC} : simulations v.s. theory

The difference observed between Fig. 1's left panel and the theoretical time spent in CC at the

⁵Cells tend to get a bit lighter as g increases however, this is likely due to noise in simulations, as when g grows payoffs become undifferentiated.

pseudo-equilibrium (displayed in Fig. 1’s right panel) can be interpreted as the effect of the basin of attraction of the ω_{DD} -equilibrium. Depending on the values of ε and g , this difference is more or less important. It is particularly striking for low value of g and low values of ε . This denotes an important variation of the size of the basin of attraction of the pseudo-equilibrium with respect to those variables.

6.3 Measuring $\lambda(\mathcal{B}(\varepsilon_A, \varepsilon_B, g))$

In this section, our objective is to find a method to measure the size of the basin of attraction of spontaneous coupling in order to distinguish its effect on τ_{CC}^g from the length and frequency of periods spent in ω_{CC} . For this purpose, we perform two distinct clustering tasks using a simple K-means algorithm [25, 17] with two clusters ($K=2$).

K-means is a well-known algorithm used to perform unsupervised learning. Given a set of points in a space, it aims at assigning *observations*, points in a metric space, to clusters, which form a partition of the set of observations. The quality of a clustering is measured with an inertia metric. Formally, given (E, d) a metric vector space, $X = \{X_i, i \in [1, \dots, n]\}$ a set of n observations, and $C = \{C_1 \dots C_K\}$ a partition of X , the inertia metric is given by

$$I(C, X) = \sum_{i=1}^K \sum_{k=1}^{|C_i|} d(X_i, \mu_i) \quad (30)$$

where $\mu_i = \frac{1}{|C_i|} \sum_{k \in C_i} X_k$ is the *barycenter* of cluster C_i . Even though K-means is known to perform good for simple tasks, it is a heuristic method that does not necessarily produce the best clustering. Given the simplicity of our task, we do not look for more advanced methods of clustering. The algorithm takes as input a list of observations, in our case a list of 4-dimensional points, and a number of clusters (in our case $K = 2$), and outputs the centers of the identified clusters as well as the cluster to which each observation belongs, which enables to compute the inertia metric of the achieved clustering. It proceeds as follows: first, it chooses randomly K observations as clusters’ centers and produces the associated Voronoï diagram (i.e. assigns each observation to the cluster with nearest center). Then, it updates the centers of the clusters given the new partition of observations and repeats the operation. The process stops whenever the clusters’ centers do not move anymore.

In the first task, we measure τ_{CC}^g by counting the number of periods algorithms spend in ω_{CC} once they have reached their limiting behavior, and then classify triplets of parameters into two categories, either allowing for spontaneous coupling or not, using τ_{CC}^g as a feature. The algorithm successfully identifies one cluster with low values of τ_{CC}^g and another with higher values, the second being the triplets of parameters allowing for spontaneous coupling. Then, for triplets of parameters for which spontaneous coupling is detected, we simulate k runs (either

$k = 100$ or $k = 1000$ depending on the computational intensity of the experiments) of our Q-learning algorithms, get the limiting Q-values and use them in a similar clustering task. More information about the clustering tasks performed is available in Appendix. Once the clusters are identified, we count how many of the runs ended up in each cluster to get a measure of $\lambda(\mathcal{B}(\varepsilon_A, \varepsilon_B, g))$. We show the outcome of our measurements in Fig. 2.

Our results indicate that, for a given g , spontaneous coupling appears for moderate values of ε_A and ε_B . In line with Banchio and Mantegazza (2023) 's results, this region enlarges when g increases, covering 0% of the square $(\varepsilon_A, \varepsilon_B) \in [0, 1]$ in the case $g = 1$ up to 80% of it when $g = 2$. Interestingly, no spontaneous coupling is detected at all for values of g below 1.4, which contradicts the theoretical result of Banchio and Mantegazza (2023). This might be due to our detection method, but in any case, our simulations indicate that spontaneous coupling is reached with negligible probability ($\lambda(\mathcal{B}(\varepsilon_A, \varepsilon_B, g)) \approx 0$) when g is too low. Also, we note that within the existence region, the effect of $(\varepsilon_A, \varepsilon_B)$ is relatively small. Particularly when g is high, most of the parameters allowing for spontaneous coupling feature a negligible probability to end up in the DD steady-state ($\lambda(\mathcal{B}(\varepsilon_A, \varepsilon_B, g)) \approx 1$). Finally, we note that asymmetry *per se* is detrimental to spontaneous coupling as $\lambda(\mathcal{B}(\varepsilon_A, \varepsilon_B, g))$ is typically lower when ε_A and ε_B are very different. In such cases, for example if $\varepsilon_A \gg \varepsilon_B$, under spontaneous coupling, A often defects in the ω_{CC} periods causing Q-values of B for action C not to increase enough. Indeed, for spontaneous coupling to be sustained, more favorable (i.e. higher) initial conditions for Q_C should be chosen, thus reducing $\lambda(\mathcal{B}(\varepsilon_A, \varepsilon_B, g))$.

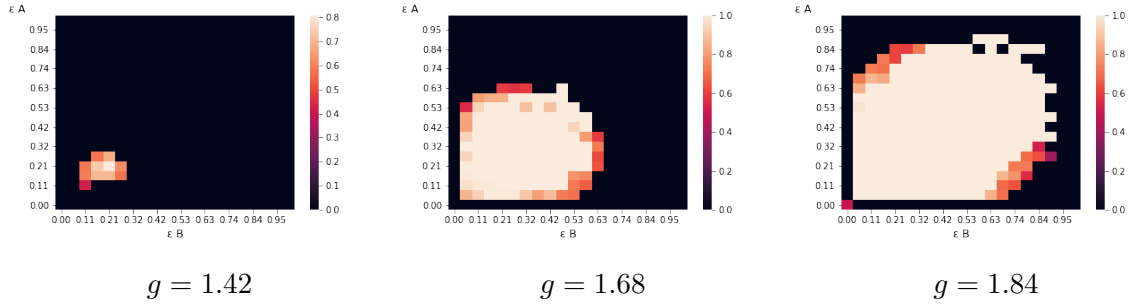


Figure 2: $\lambda(\mathcal{B}(\varepsilon_A, \varepsilon_B, g))$ on heatmaps for different values of g

6.4 Time spent in each region under spontaneous coupling

Under spontaneous coupling, algorithms alternate between phases of mutual cooperation, mutual defection and asymmetric behavior. In this section, we aim at measuring these times as functions of $\varepsilon_A, \varepsilon_B$ and look at the specific case $g = 1.7$. In order to do so, for one couple $(\varepsilon_A, \varepsilon_B)$ we simulate the process $k = 100$ times for $T = 10^5$ periods each and save the Q-values for the last 1000 periods. We are able to get the frequency with which a transition from a region to another happens, as if the process were Markovian with respect to its being in $\omega_{CC}, \omega_{CD}, \omega_{DC}$ or ω_{DD} . In particular, we measure the probability with which the system

remains in ω_{CC} (i.e. the probability of a ω_{CC} to ω_{CC} transition conditional on being in ω_{CC}), the probability with which it remains in ω_{DC} and the probability of a ω_{CC} to ω_{CD} transition to happen conditional on a transition from ω_{CC} to $\omega_{CD} \cup \omega_{DC}$ to happen. The first two give a sense of how long the ω_{CC} and ω_{CD} phases are, while the third one indicates with which frequency an asymmetric transition is beneficial to player B . These measures are represented using in Fig. 3. Results indicate that the length of cooperative periods is monotonic with respect to

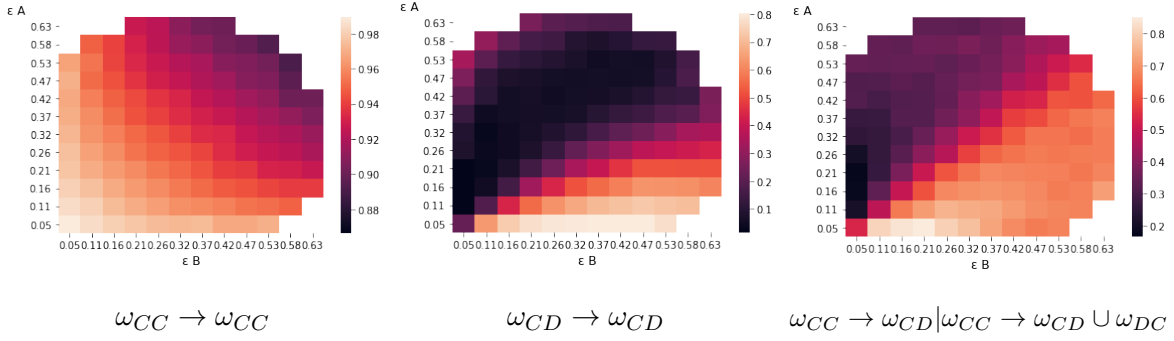


Figure 3: Transitions probabilities for $g = 1.7$

each ε : an increase in one's own exploration parameter is always harmful to cooperation in the sense that the system will spend less time in ω_{CC} and more time in either ω_{DD} or in asymmetric regions. This is coherent with the intuition we gave to spontaneous coupling: when ε is higher, the Q-value for D is updated more often in the ω_{CC} phases, causing it to increase faster and eventually to get above that of C quicker. The transition from ω_{CD} to ω_{CD} (second heatmap of Fig. 3) gives us the following information. When $\varepsilon_A > \varepsilon_B$, the time spent in ω_{CD} is quite short and almost constant, whereas in the other part of the heatmap, it is longer, increasing in ε_B and decreasing in ε_A . We give this the following explanation. When the system is in ω_{CD} , then previously it was most probably in ω_{CC} . The transition from ω_{CC} to ω_{CD} happened as B was quicker to realize that D yields a higher payoff. Until A realizes this fact too, the system remains in ω_{CD} . Thus, in the bottom right part of the heatmap, when ε_B increases, B gets further ahead of A in realizing action D is dominant, while when ε_A increases, A is quicker to catch up with B . When $\varepsilon_A > \varepsilon_B$, the system spends time in ω_{CD} somehow "by accident" and not as a natural transition from ω_{CC} . Being due to the inherent noise of the system, it is weakly affected by exploration parameters. Finally, the third heatmap of figure 3 generally confirms the interpretation given for the second one, though we note a non-monotony with respect to ε_B in the bottom right part which we could not explain so far. It appears consistently for different values of ε_A and g so that it is probably not due to measurement errors nor noise in the process. Surprisingly, for a given value of ε_A there seems to be an intermediate value of ε_B such that the system enters ω_{CD} rather than ω_{DC} with highest probability.

6.5 Vizualizing $\tau_{X,Y}^g$

Total time spent in each region can be measured using the same simulation results, by counting how many of the last 1000 periods are spent in each region. This yields a result aggregating both the effect of $\lambda(\mathcal{B}(\varepsilon_A, \varepsilon_B, g))$ and of the length of periods inside specific regions. We represent the outcome in Fig. 4. The time spent in ω_{CC} is non-monotonic, and tends to be higher when exploration parameters are low and symmetric. We do not really observe this non-monotony for ω_{DD} , except at the boundaries of the existence region, which corresponds to the effect of exploration policies on the basin of attraction of spontaneous coupling discussed in section 6.3. Finally, we point that the time spent in symmetric regions (either ω_{CD} or ω_{DC}) increases with the difference between ε_A and ε_B . We give the following interpretation for these results. Say $\varepsilon_A > \varepsilon_B$. When the system is in ω_{CC} , it will most likely transition to an asymmetric region, either ω_{CD} or ω_{DC} . As stated earlier, the algorithm with highest exploration policy will realize quicker that D is a dominant action, causing a transition to ω_{DC} in our case (A is quicker to realize that D is dominant). Thus, the time spent in ω_{CC} really depends on the *highest* exploration policy: the lower this quantity, the longer the time spent in ω_{CC} . This explains the non-monotony observed for ω_{CC} . Once the system has entered a non-symmetric region, the algorithm holding D as a preferred action (in our case, A) has no reason to switch its preference to C as it is exploiting the other's cooperative behavior. The other however, needs to realize that C is dominated. Hence, the higher ε_B and thus the closer to ε_A , the smaller the time spent in ω_{DC} , which explains the shape of Fig. 4's third panel. Finally, the fact that, contrarily to ω_{CC} , time spent in ω_{DD} is monotonic with respect to both exploration parameters can be explained by the fact that increasing one's level of exploration increases the time spent in ω_{DD} in two regards. Increasing the highest exploration level leads to a shorter ω_{CC} phase, and thus mechanically to a longer ω_{DD} one, but it also leads to a shorter asymmetric phase, producing the same effect.

These three observations together indicate that when the player holding the highest exploration parameter decides to unilaterally increase it, the time taken from τ_{CC}^g is spent in an asymmetric region rather than in τ_{DD}^g . The effect of one player's exploration parameter on τ_{CC}^g is thus non-monotonic, and ε s should be equal in order for τ_{CC}^g to be maximized.

7 General equilibria of $G(g)$

In this section we turn our attention to $G(g)$ and its equilibria. We have proven in section 5 that $(0, 0)$ is always a Nash equilibrium, now we aim at numerically finding other equilibria by using our simulations and to see how they are affected by g .

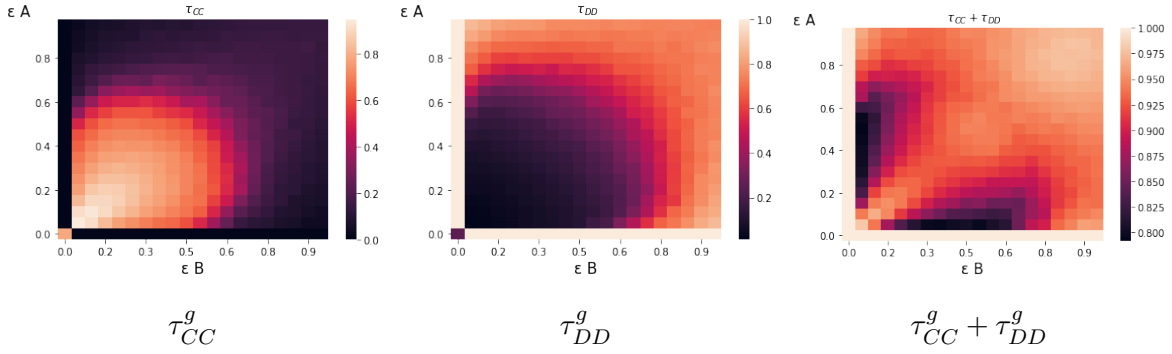


Figure 4: $\tau_{X,Y}^g$ for $g = 1.7$

7.1 Best response functions: shapes and interpretation

We first generate the best response functions and analyze their shapes. Figure 5 displays the

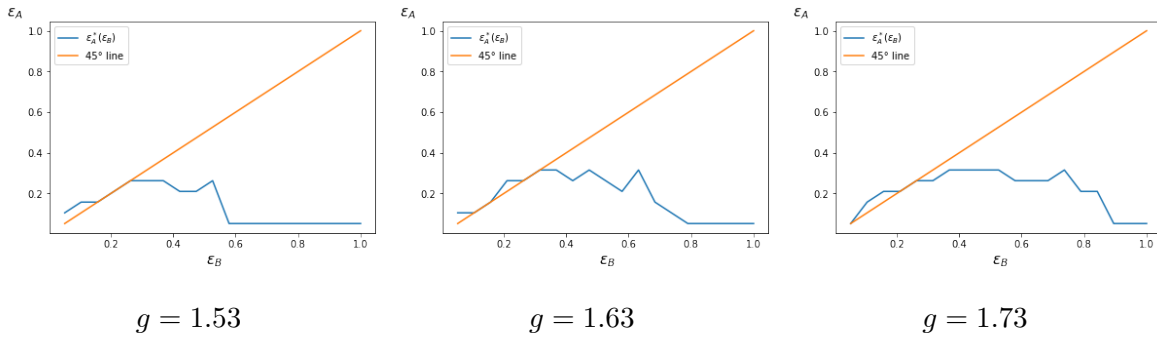


Figure 5: Best response functions for different values of g

shapes of best response functions for three different values of g . Although the result is pretty noisy (due to noise in the payoff matrix generation method), the curves all share a common pattern: there is a first phase during which it is increasing and follows the 45° line, followed by a decreasing phase which ends up in it being flat and equal to 0. The last portion is straightforward to interpret: when ε_B is big, the chance to end up in ω_{DD} is high regardless of ε_A . Thus, a best response for A is to set his exploration policy to 0: otherwise, A will be playing C with some probability, while C is dominated by D . Note that the length of the flat part is decreasing in g .

Conditional on being in a cooperative pseudo-equilibrium with enough time spent in the cooperative region, exploration allows to exploit the other. Indeed, when in ω_{CC} , raising one's exploration level allows to play D more often during this period of time and thus to make higher payoff. However, this is payoff reducing when in ω_{DD} : in this case the situation is reversed, as adopting high exploration causes to play C more often while the other player plays D . On top of this, we have seen in section 6.5 that increasing one's exploration when it is higher than the other player's has the effect of reducing τ_{CC}^g and to increase τ_{DD}^g . Thus, when setting an exploration level above that of the opponent, players cannot choose one that is too high. As

τ_{DD}^g and ε increase, raising the exploration level becomes counterproductive. In an extreme case in which an agent were to increase his exploration level too much, he would simply break the spontaneous coupling. We can consider the most extreme case to illustrate. A would like to have his exploration level set at 1 if he had the guarantee that algorithms will remain in the cooperative pseudo-equilibrium. However we have seen that this would cause the system to go to ω_{DD} for sure (Proposition 4. Thus, if A chooses $\varepsilon_A = 1$, he is sure to drive the system in ω_{DD} while having a high exploration level in ω_{DD}). When ε_B increases, for a given ε_A , the time spent in ω_{DD} as well as the risk of breaking the pseudo-equilibrium increase, so that the best response functions are eventually flat for large ε_B . Note how, when g increases, the flat part of the curve begins for higher values of ε_B , which is clearly related to higher g allowing for spontaneous coupling for larger exploration policies.

An additional mechanism needs to be added to understand why the best response functions are increasing at first for moderate values of ε_B . When ε_B is above ε_A , increasing ε_A has two effects. First, it increases the time spent in ω_{CC} which is beneficial to A , especially since she is increasing her exploration policy. Second, it allows to reduce the time spent in ω_{CD} and to eventually (when ε_A gets higher than ε_B) increase the time spent in ω_{DC} . This feature is of clear strategic interest, as during the time spent in this region, she will be playing D more often while B will be playing C more often, allowing to collect higher payoff by *exploiting* the other's cooperation. Now, starting from ω_{CC} , agents will most likely go to ω_{CD} or ω_{DC} , the quickest, i.e. generally the one with the highest exploration policy, wins the race and gets into a favorable position. As we have seen with our simulation results in Section 6.4 though, there is a non-monotony making this mechanism non-trivial.

8 Equilibrium results

8.1 Method

The game we consider is symmetric. We can thus find Nash equilibria by finding the intersection of the best response functions with their symmetric with respect to the 45° line. This method allows us to get, for each g , Nash equilibria (symmetric and non symmetric) as well as Pareto optimal profiles. The generation of the best response functions is noisy in essence and so will be the equilibria. Thus we only seek to interpret their general pattern and how they are affected by g . Figure 6 shows the result of the identification of equilibria for different values of g . The left panel displays Pareto optimal profiles, as well as equilibria, which we find to be all symmetric. They are all plotted on the previously studied heatmap in order to know whether they are in regions allowing for cooperation or not. This allows us to quickly identify, for a given equilibrium, the level of coupling attained. To discriminate the equilibria appearing because of noise, we use the following method. We generate perturbed payoff matrices

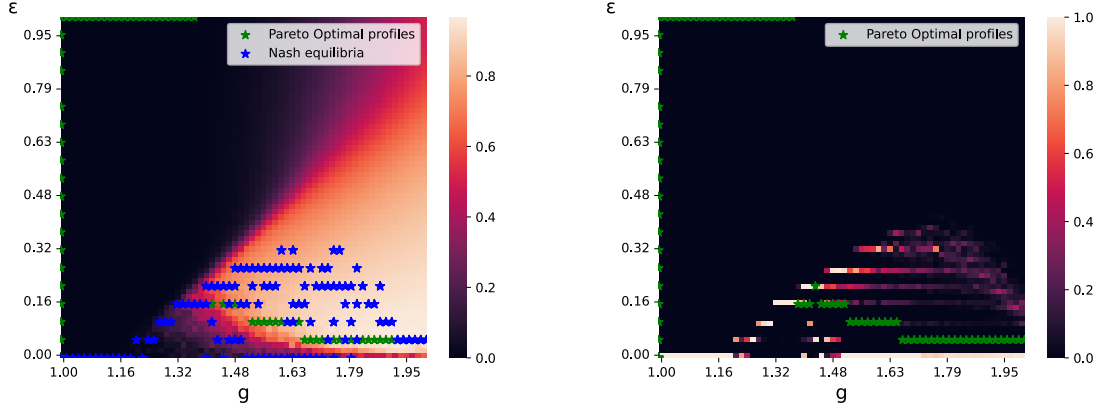


Figure 6: Left panel: Nash equilibria and Pareto optima displayed on the learned-action heatmap Right panel: Nash-equilibria frequency heatmap.

($M = 1000$) by adding a small noise to the original payoff matrices and compute equilibria. Then for each cell of right panel’s heatmap, we measure the frequency with which a Nash equilibrium appears in the perturbed payoff matrices. Results indicate that $(0, 0)$ is almost always a Nash equilibrium, and that equilibria found with highest frequency lie on a bell-shaped curve.

8.2 Nash equilibria

Fig. 6 shows that $\varepsilon_A = \varepsilon_B = 0$ often comes out as an equilibrium, in conformity with Proposition 5. However many other equilibria exist, in particular when g is high enough. When a symmetric profile allowing for a good level of exploration exists (i.e. when some cells of the heatmap have a light color) it is notable that equilibria tend to be located inside the region, which confirms the existence of highly cooperative Nash equilibria in line with Proposition 5.

When g is small, the only Nash equilibrium is the $(0, 0)$ one. This relates to the basin of attraction of spontaneous coupling being negligible for g too small. In this case, the best response functions are constantly equal to 0 so that the only equilibrium is $(0, 0)$. Figure 6 also shows that, as g increases, the equilibrium with highest exploration level first tends to increase until g reaches intermediate values and then decreases. An explanation for this can be the following trade-off. When g is low, exploration is very costly as it is very likely to break the pseudo-equilibrium. As g increases, agents have more latitude in choosing a high exploration policy. However, the attractiveness of exploration tends to decrease with g . Indeed, exploring in the case of a pseudo-equilibrium enables players to play D instead of C . Thus, when the opponent is playing C , instead of making $2g$, a player will be getting $2 + g$, and when the opponent plays D , he gets 2 instead of g : the net benefit of playing D over C is thus always $2 - g$, so that the incentive to deviate from mutual cooperation tends to decrease. Because of this, as g increases, there is a tendency to prefer cooperative outcomes. Those conflicting tendencies are

an explanation of the shape we observe for the distribution, our guess being that, as g grows larger the reduction in the incentive to play D instead of C exceeds the effect on the robustness of spontaneous coupling to high level of exploration.

8.3 Pareto optimal profiles

Our simulations indicate that all Pareto optimal profiles are symmetric. This is a consequence of symmetric profiles minimizing the time spent in $\omega_{CD} \cup \omega_{DC}$, which is harmful in terms of joint payoff. Additionally, τ_{CC} increases when the highest exploration parameter is reduced. Thus, for any couple of asymmetric exploration parameters with $\varepsilon_A > \varepsilon_B$, under the profile $(\varepsilon_B, \varepsilon_B)$ the time spent in $\omega_{CD} \cup \omega_{DC}$ as well as the time spent in ω_{DD} are reduced, while the time spent in ω_{CC} is increased, which increases the joint output. The distribution of Pareto optimal profiles can be interpreted as follows. To maximize social surplus, there is a trade-off. Increasing the exploration level gives a benefit for the periods in which D is held as a preferred action, and is costly in the other case. On top of this, it is socially better to choose low exploration policies in order to maximize time spent in ω_{CC} . As g increases, for a given profile, the time spent in ω_{DD} tends to decrease, and thus the social benefit to choose a high exploration policy decreases. This explains the generally decreasing shape of the distribution of Pareto optimal profiles. When g is too low, the time spent in ω_{CC} is virtually 0 no matter the exploration policy, so that the socially optimal profile is to choose $\varepsilon_A = \varepsilon_B = 1$. Note also how Pareto optima get steady for high values of g , yet above 0. This can be related to minimal exploration being required in order to maximize the probability of reaching spontaneous coupling as our results of Section 6.3 have shown. Also, in the second part of the distribution (for values of g in which some time is actually spent in ω_{CC}), we note that Pareto optimal values of exploration are typically lower than equilibrium ones, i.e. agents tend to over-explore. This reveals how there is an incentive to unilaterally increase the exploration level when spontaneous coupling appears with a high enough probability so as to often play D when the other is playing C in order to get $2 + g$ rather than $2g$. Our guess is that this difference between Pareto optimal profiles and Nash equilibria is limited by the effect player's individual exploration parameter have on the time spent in τ_{CC} . If this is the case, it should intuitively be increased when there are more players involved. Interestingly though, when g is large enough, at Nash equilibria profiles cooperation is more often *learned* than at Pareto profiles. This seemingly paradoxical fact is due to ε controlling for both the time spent in ω_{CC} and the frequency with which C is played inside this region. At the equilibria profiles, cooperation is learned more often but played less often than at Pareto optimal profiles because of ε being higher.

9 Conclusion

In this paper, we have defined and studied a *designing game* in which strategically chosen algorithms repeatedly play a prisoner’s dilemma on behalf of players. We have provided evidence that a mechanism responsible for algorithmic collusion, *spontaneous coupling*, persists by allowing different exploration policies. We have shown that this mechanism persists in equilibrium, and is thus robust to competition over the algorithms’ parameterization. The essential trade-off to retain from our analysis is between the incentive to increase one’s exploration policy in order to exploit the other players during the time spent in ω_{CC} , and the risk of breaking the spontaneous coupling high exploration policies imply, which is detrimental to players. As players are able to guarantee themselves the best possible situation in a non-cooperative outcome by setting their exploration level equal to zero, in equilibrium, there is no room for situations including coupling that would be very detrimental to one of the players. This gives insight on the difference between equilibrium profiles and Pareto ones, indicating that competition between algorithms potentially decreases the degree of collusion. Further, our simulations shed light on more involved mechanisms regarding time spent in asymmetric regions: a player might want to raise his exploration level above the one of his opponent in order to benefit from time spent in positively asymmetric situation. By doing so, one’s algorithm realizes quicker than the other that D is a dominant strategy and benefits from his opponent’s slowness. This however comes at the risk of transitioning too fast from DD phases to a negatively asymmetric phase.

Our results call for further work. In particular, we chose to focus on exploration policies since they have a straightforward interpretation in terms of exploration and exploitation. A similar analysis could well be applied to the learning rate α , which we left exogenously fixed, as well as to the initial conditions, which could be regarded as parameters of the algorithms and thus chosen beforehand by players. In particular, we believe that further work on initial conditions is needed so as to better understand algorithmic interactions and to get stronger results. Also, our findings suggest that competition makes equilibrium exploration levels higher than Pareto ones, so that in a sense, collusion is weakened by competition between algorithms. An interesting direction could be to extend the model to more than two Q-learning algorithms. Our intuition is that, by decreasing the impact each algorithm individually has on the system as a whole, the cost of exploration decreases while it remains beneficial. We thus expect spontaneous coupling to disappear when the number of agents is large.

Appendices

A Proof of mathematical results

Proof of Proposition 1. When action X is chosen by player i at time t , its Q-value is updated as follows:

$$Q_i^X(t+1) = (1-\alpha)Q_i^X(t) + \alpha \left[\gamma \max_{X' \in \{C, D\}} Q_i^{X'}(t) + r_X^i(t) \right], \quad (31)$$

where $r_X^i(t)$ is the (stochastic) reward received by player i at t . This reward has two possible values: $\tilde{\pi}_{X,D}^i$ and $\tilde{\pi}_{X,C}^i$, which are such that $\tilde{\pi}_{X,C}^i \geq \tilde{\pi}_{X,D}^i$. One can rewrite the above equation and get:

$$\Delta(Q_i^X)(t) \equiv Q_i^X(t+1) - Q_i^X(t) = \alpha \left[r_X^i(t) - (Q_i^X(t) - \gamma \max_{X'} Q_i^{X'}(t)) \right], \quad (32)$$

so that there are two cases:

$$\frac{1}{\alpha} \Delta(Q_i^X)(t) = \begin{cases} r_X^i(t) - (Q_i^X(t) - \gamma \max_{X'} Q_i^{X'}(t)) & \text{if } X \neq \arg \max_{X'} Q_i^{X'}(t). \\ r_X^i(t) - (1-\gamma)Q_i^X(t) & \text{if } X = \arg \max_{X'} Q_i^{X'}(t). \end{cases} \quad (33)$$

Note that in both cases:

$$\frac{1}{\alpha} \Delta(Q_i^X)(t) \geq r_X^i(t) - (1-\gamma)Q_i^X(t) \quad (34)$$

So that if $Q_i^X(t) < \frac{\tilde{\pi}_{X,D}^i}{1-\gamma}$:

$$\frac{1}{\alpha} \Delta(Q_i^X)(t) \geq \tilde{\pi}_{X,D}^i - (1-\gamma) \frac{\tilde{\pi}_{X,D}^i}{1-\gamma} = 0. \quad (35)$$

Thus, if $Q_i^X(t)$ is below $\frac{\tilde{\pi}_{X,D}^i}{1-\gamma}$, it grows. Now, assume for some t , $Q_i^X(t) \geq \frac{\tilde{\pi}_{X,D}^i}{1-\gamma}$, then:

$$\begin{aligned} Q_i^X(t+1) &= (1-\alpha)Q_i^X(t) + \alpha \left[\gamma \max_{X'} Q_i^{X'}(t) + r_X^i(t) \right] \\ &\geq (1-\alpha) \frac{\tilde{\pi}_{X,D}^i}{1-\gamma} + \alpha \left[\gamma \frac{\tilde{\pi}_{X,D}^i}{1-\gamma} + \tilde{\pi}_{X,D}^i \right] \geq \frac{\tilde{\pi}_{X,D}^i}{1-\gamma}. \end{aligned} \quad (36)$$

It is then clear that, with probability 1, there exists t^* such that for all $t > t^*$, for all $i \in \{A, B\}$ and for all $X \in \{C, D\}$, $Q_i^X \geq \frac{\tilde{\pi}_{X,D}^i}{1-\gamma}$.

Now assume that for some $X \in \{C, D\}$, $Q_i^X(t) > \frac{2+g}{1-\gamma}$. There are two cases:

- If $X^* = \arg \max_{X'} Q_i^{X'}(t)$ is chosen at t , then:

$$\Delta(Q_i^{X^*})(t) = \alpha \left[r_X^i(t) - (1-\gamma)Q_i^{X^*}(t) \right] < 0, \quad (37)$$

and for $X \neq X^*$, Q_i^X is unchanged.

- If $X \neq \arg \max_{X'} Q_i^k(t)$ is chosen at t , then:

$$\begin{aligned} Q_i^X(t+1) &= (1-\alpha)Q_i^X(t) + \alpha \left[\gamma \max_{X'} Q_i^{X'}(t) + \tilde{\pi}_X^i(t) \right] \\ &\leq (1-\alpha) \max_{X'} Q_i^X(t) + \alpha \left[\gamma \max_{X'} Q_i^{X'}(t) + (1-\gamma) \max_{X'} Q_i^{X'} \right] \\ &\leq \max_{X'} Q_i^X(t). \end{aligned} \quad (38)$$

Thus, if one of the Q-values is above $\frac{2+g}{1-\gamma}$, the maximum of Q-values needs to decrease. Then if it is the case, for sure for some t further in time $\max_{X'} Q_i^{X'}(t') \leq \frac{2+g}{1-\gamma}$. For such t' , for all i, X :

$$Q_i^X(t+1) \leq (1-\alpha) \frac{2+g}{1-\gamma} + \alpha(2+g) + \alpha\gamma \frac{2+g}{1-\gamma} = \frac{2+g}{1-\gamma}. \quad (39)$$

Then clearly, with probability 1, there exists t'^* such that for all $t > t'^*$, for all i, X , $Q_i^X \leq \frac{2+g}{1-\gamma}$. Now, assume for some i , and for some $t > \max(\{t^*, t_1^*\})$, $Q_i^C(t) \in]\frac{2g}{1-\gamma}, \frac{2+g}{1-\gamma}]$. Consider a specific sequence of plays such that: i 's opponent always plays D , and i always plays the action with highest Q-value. The probability of such sequence of plays of length L is higher than $\left(\frac{\epsilon_j}{2}(1-\epsilon_i)\right)^L$. In this case, in each step, the Q-value of the updated action decreases at least by αg if C has the highest Q-value, and at least by $2\alpha(g-1)$ if D has the highest Q-value. Thus, any such sequence of length

$$L = \left\lceil \frac{2}{1-\gamma} \frac{1}{2\alpha(g-1)} \right\rceil \quad (40)$$

is guaranteed to drive Q_i^C below $\frac{2g}{1-\gamma}$. Reiterating this process with the other player in the case he has a Q-value for C higher than $\frac{2g}{1-\gamma}$ yields the same result. Since this happens with strictly positive probability, we know that with probability 1, the Q values will be in the desired interval at some point in time. \square

Proof of Proposition 2. This result is simply obtained by setting the flow of the continuous time approximation in ω_{DD} to $(0, 0, 0, 0)$. For $(X, Y) \neq (D, D)$ non-existence is obtained by setting the flow in $\omega_{X,Y}$ to $(0, 0, 0, 0)$ and observing the solution does not lie in $\omega_{X,Y}$. \square

Proof of Proposition 3. In this case, for any $(X, Y) \in \{C, D\}^2$, the dynamics within $\omega_{X,Y}$ solve:

$$\begin{cases} \dot{Q}_A^X(t) = \frac{\alpha}{2} \left[\hat{\pi}_{X,Y} - (1-\gamma)Q_A^X(t) \right] \\ \dot{Q}_A^{-X}(t) = \frac{\alpha}{2} \left[\hat{\pi}_{-X,Y} + \gamma Q_A^X(t) - Q_A^{-X}(t) \right]. \end{cases} \quad (41)$$

Taking the difference between the two equations allows us to get a differential equation for

$\Delta(Q_A^X)(t)$:

$$\Delta(\dot{Q}_A^X)(t) + \frac{\alpha}{2}\Delta(Q_A^X)(t) = \frac{\alpha}{2}(\hat{\pi}_{X,Y} - \hat{\pi}_{-X,Y}). \quad (42)$$

This equation has a simple solution of the form:

$$\Delta(Q_A^X)(t) = K_0 \exp(-\alpha t) + (\hat{\pi}_{X,Y} - \hat{\pi}_{-X,Y}), \quad (43)$$

so that $\Delta(Q_A^X)$ is monotonic and:

$$\begin{cases} \Delta(Q_A^X)(0) \geq 0 \text{ by definition} \\ \lim_{+\infty} \Delta(Q_A^X)(t) = \hat{\pi}_{X,Y} - \hat{\pi}_{-X,Y}. \end{cases} \quad (44)$$

Since $\hat{\pi}_{X,Y} - \hat{\pi}_{-X,Y} > 0$ when $X = D$ and $\hat{\pi}_{X,Y} - \hat{\pi}_{-X,Y} < 0$ when $X = C$, it is clear that whenever player A enters D it remains in D , and eventually exits C to D when it is in C . Thus, no matter the initial condition:

$$\exists t^* \text{ s.t. } \forall t > t^*, Q_A^D(t) > Q_A^C(t). \quad (45)$$

Now, we can focus on the Q values of player B , fixing the behavior of A to be stationary. This defines a dynamic system on its own, characterized by the piece-wise linear dynamics of player B 's Q values. We proceed by contradiction, assuming that there is a pseudo equilibrium for this system. The linear dynamics in each continuity domain follow:

$$\vec{F}_{DC}^B = \begin{pmatrix} \alpha(1 - \frac{\varepsilon_B}{2}) \left[\frac{g}{2} + g + \gamma Q_B^D(t) - Q_B^C(t) \right] \\ \alpha \frac{\varepsilon_B}{2} \left[\frac{2+g}{2} + 1 - (1 - \gamma) Q_B^D(t) \right] \end{pmatrix}, \quad (46)$$

$$\vec{F}_{DD}^B = \begin{pmatrix} \alpha \frac{\varepsilon_B}{2} \left[\frac{g}{2} + g - (1 - \gamma) Q_B^C(t) \right] \\ \alpha \frac{\varepsilon_B}{2} \left[\frac{2+g}{2} + 1 + \gamma Q_B^C(t) - Q_B^D(t) \right] \end{pmatrix}. \quad (47)$$

Let $\vec{N} = \begin{pmatrix} 1 \\ -1 \end{pmatrix}$ the normal vector to $A = \left\{ \begin{pmatrix} x \\ x \end{pmatrix}, x \in \mathbb{R} \right\}$. Under our hypothesis, there exists τ^* such that:

$$\tau^* \vec{F}_{DC}^B|_{Q_B^D=Q_B^C} + (1 - \tau^*) \vec{F}_{DD}^B|_{Q_B^D=Q_B^C} = 0, \quad (48)$$

and

$$\tau^* F_{DC}^B|_{Q_B^D=Q_B^C} + (1 - \tau^*) F_{DD}^B|_{Q_B^D=Q_B^C} = \vec{0}. \quad (49)$$

Solving the first equation for τ^* we get

$$\tau^* = \frac{2Q_B(1 - \gamma)(1 - \varepsilon_B) + 2\varepsilon_B(g + 1) - (g + 4)}{4(1 - \varepsilon_B)\left((1 - \gamma)Q_B - (g + 1)\right)} \quad (50)$$

which we substitute in the second and get:

$$\frac{\alpha(3g - 2(1 - \gamma)Q_B)(4 + g - 2(1 - \gamma)Q_B)}{8(1 + g - (1 - \gamma)Q_B)} \begin{pmatrix} 1 \\ 1 \end{pmatrix} = \vec{0}, \quad (51)$$

which has two solutions:

$$Q_B = \frac{3g}{2(1 - \gamma)} \text{ or } Q_B = \frac{4 + g}{2(1 - \gamma)}. \quad (52)$$

This gives two possibilities for τ^* :

$$\tau^* = \frac{2 - \varepsilon_B}{2(1 - \varepsilon_B)} > 1 \text{ or } -\frac{\varepsilon_B}{2(1 - \varepsilon_B)} < 0. \quad (53)$$

This final line gives us a contradiction. \square

Proof of Proposition 4. First we focus on the Q-values of player A . Since $\varepsilon_A = 0$, in each period, A only updates the highest Q-value. Thus, if X is updated at t :

$$\Delta(Q_A^X(t)) = \alpha \left[r_X^i(t) - (1 - \gamma)Q_A^X \right] \geq 0 \iff Q_A^X(t) \leq \frac{r_X^i(t)}{1 - \gamma}. \quad (54)$$

As a consequence, when $Q_A^X(t) \in [\frac{\tilde{\pi}_{X,D}^i}{1 - \gamma}, \frac{\tilde{\pi}_{X,C}^i}{1 - \gamma}]$, when updated, it grows when the reward received is high (i.e. when the opponent plays C) and it decreases when the reward received is low (i.e. when the opponent plays D). Note also that:

$$Q_A^X(t) \in [\frac{\tilde{\pi}_{X,D}^i}{1 - \gamma}, \frac{\tilde{\pi}_{X,C}^i}{1 - \gamma}] \implies Q_A^X(t + 1) \in [\frac{\tilde{\pi}_{X,D}^i}{1 - \gamma}, \frac{\tilde{\pi}_{X,C}^i}{1 - \gamma}]. \quad (55)$$

Let $Q_A^C(t)$ and $Q_A^D(t)$ in $[\frac{2}{1 - \gamma}, \frac{2g}{1 - \gamma}]$. Any other situation can be proven to lead to this case. We prove that, with probability 1, Q_A^C goes under $\frac{2}{1 - \gamma}$, in which case, for sure, Q_A^D will remain higher than Q_A^C onward.

Let a realization of rewards such that for all t , $Q_A^C \in [\frac{2g}{1 - \gamma}, \frac{2}{1 - \gamma}]$. Consider a sequence of consecutive low rewards of length L . Along such a sequence, the Q values, when updated, decrease. More precisely:

$$\forall t \text{ s.t. } Q_A^X(t) > Q_A^{-X}(t), Q_A^X(t + 1) = \left(1 - (1 - \gamma)\alpha\right) Q_A^X(t) + \alpha \underline{\pi}_A^X. \quad (56)$$

For T^X a set of consecutive integers such that $\forall t \in T^X, Q_A^X(t) > Q_A^{-X}(t)$, by denoting T_0 the first of them we get that:

$$\forall t \in T^X, Q_A^X(t) = \left(1 - (1 - \gamma)\alpha\right)^t \left(Q_A^X(T_0) - \underline{\pi}_A^X\right) + \frac{\underline{\pi}_A^X}{1 - \gamma}. \quad (57)$$

We can also extract from the sequence $(Q_A^X)_{t \in \mathbb{N}}$ the sequence $(Q_A^X)_{t \in \cup T_X}$ and relabel time such that for all k , t_k^* designates the k -th period of time at which action X was updated. By the way, it is clear that by allowing L large enough, we can get as many such periods of time as we want. Then one can note that:

$$\lim_{t_C^* \rightarrow \infty} Q_A^C(t_C^*) = \frac{g}{1-\gamma} < \frac{2}{1-\gamma} \quad (58)$$

so that there exists a finite t_k^* such that $Q_A^C(t_C^*) < \frac{2}{1-\gamma}$. Thus for any initial condition, by choosing L large enough but finite, a sequence of L consecutive low rewards leads to Q_A^C exiting the interval. Note as well that the number of updates of C necessary for this is biggest when $Q_A^C(0)$ is highest, thus there exists L such that our previous result holds for any initial condition. Thus, whenever the Q values of A lie in the interval $[\frac{2g}{1-\gamma}, \frac{2}{1-\gamma}]$, if a large enough (but finite) sequence of low rewards happens, Q_A^C will exit the interval. If we assume the Q values remain inside for an infinite number of periods, then Q_A^C exits with probability 1. Finally, we conclude that, with probability 1, there exists t such that for any $t' > t$, $Q_A^C(t) < \frac{2}{1-\gamma}$. By a similar reasoning than in Proposition 3, we get that spontaneous coupling is not possible. \square

Proof of Proposition 5. First, note that if for some t , $\mathbb{Q}(t) \in \omega_{CC}$, then for all subsequent t' , $\mathbb{Q}(t') \in \omega_{CC}$. Then, for any initial condition starting the process in ω_{CC} , the system will stay in ω_{CC} . This happens with probability:

$$\mathbb{P}(\mathbb{Q}_0 \in CC) = \mathbb{P}\left(Q_A^C(0) < Q_A^D(0)\right) \mathbb{P}\left(Q_B^C(0) < Q_B^D(0)\right) = \mathbb{P}\left(Q_A^C(0) < Q_A^D(0)\right)^2, \quad (59)$$

where:

$$\mathbb{P}\left(Q_A^C(0) < Q_A^D(0)\right) = \int_{\frac{g}{1-\gamma}}^{\frac{2g}{1-\gamma}} \left(\frac{1-\gamma}{g}\right)^2 \left(x - \frac{2}{1-\gamma}\right) dx = \frac{2}{g^2}(g-1)^2. \quad (60)$$

Now, assume that the system doesn't end up in ω_{CC} , then it must be the case that $\forall t, \mathbb{Q}(t) \in \omega_{DD} \cup \omega_{CD} \cup \omega_{DC}$. Further assume that $\forall t_0, \exists t > t_0$ such that $\mathbb{Q}_t \in \omega_{CD} \cup \omega_{DC}$. Then, it is clear that for all $X \in \{A, B\}$, $\left(Q_C^X(t)\right)_{t \in \mathbb{N}}$ is a decreasing sequence, and strictly decreases each time X holds C as a preferred action. Also, it must be the case that there is X such that $Q_C^X(t) > \frac{2}{1-\gamma}$, otherwise there is no way $Q_C^X(t) > Q_D^X(t)$. For each t such that $Q_C^X(t)$ decreases we get:

$$Q_C^X(t+1) - Q_C^X(t) = \alpha \left(g - (1-\gamma)Q_C^X(t) \right) < \alpha(g-2). \quad (61)$$

By our hypothesis, it is clear that for both A and B , $Q_C^X(t) < \frac{2}{1-\gamma}$ at some point, which is a contradiction. The first condition for allowing spontaneous coupling (i.e. the existence of an initial condition for which the continuous time approximation does not end up in $\tilde{\mathbb{Q}}_{DD}^{\text{eq}}$) can be easily verified by taking an initial condition in ω_{CC} and checking the continuous time approximation never leaves ω_{CC} . \square

Proof of Proposition 6. Assume $\varepsilon_B = 0$, then if A chooses $\varepsilon_A > 0$, by Proposition 4, the system converges to $\omega_D D$. Thus the payoff A makes by choosing $\varepsilon_A > 0$ is:

$$\pi_A(\varepsilon_A, 0) = 2\left(1 - \frac{\varepsilon_A}{2}\right) + g\frac{\varepsilon_A}{2} < 2 \quad (62)$$

while the payoff A makes when choosing $\varepsilon_A = 0$ is:

$$2(1 - \mathbb{P}(CC)) + 2g\mathbb{P}(CC) > 2. \quad (63)$$

We deduce the result by symmetry of the game. \square

Proof of Proposition 7. Let $\varepsilon_A \in]0, 1]$. If $\varepsilon_B = 1$, then we know from Proposition 3 that $(\varepsilon_A, \varepsilon_B, g)$ does not allow for spontaneous coupling and thus $\tau_{DD}^g = 1$. Thus player B will receive payoff:

$$\Pi^B(\varepsilon_A, 1) = \left(1 - \frac{\varepsilon_A}{2}\right)\frac{g+2}{2} + \frac{\varepsilon_A}{2}\frac{2g+2+g}{2} \quad (64)$$

whereas by playing $\varepsilon_B = 0$ still $(\varepsilon_A, \varepsilon_B, g)$ does not allow for spontaneous coupling and he would get payoff:

$$\Pi^B(\varepsilon_A, 0) = \left(1 - \frac{\varepsilon_A}{2}\right) \cdot 2 + \frac{\varepsilon_A}{2}(2+g), \quad (65)$$

which is clearly higher than the latter. Now assume $\varepsilon_A = 0$, then we already know from Proposition 6 that $(0, 0)$ is a strict Nash equilibrium in $G(g)$ which completes the proof. \square

Proof of Proposition 8. Let $\{\varepsilon_A, \varepsilon_B\} \in NE$. We first show that $\tau_{DD}(\varepsilon_A, \varepsilon_B) < 1$. By contradiction, assume $\tau_{DD}(\varepsilon_A, \varepsilon_B) = 1$. Then, since ε_A is a best response to ε_B :

$$\pi_A(\varepsilon_A, \varepsilon_B) \geq \pi_A(0, \varepsilon_B). \quad (66)$$

There are two cases:

- If $\varepsilon_B \neq 0$, the only possible best response is $\varepsilon_A = 0$. But then since $BR(0) = \{0\}$ we get $\varepsilon_B = 0$ which is a contradiction.
- If $\varepsilon_B = 0$, then $\varepsilon_A = 0$ by the same argument. Then $(\varepsilon_A, \varepsilon_B) = (0, 0)$, but then $\tau_{CC} > \frac{1}{4}$, which gives a contradiction.

Thus, $\tau_{DD}(\varepsilon_A, \varepsilon_B) < 1$. Now assume $\tau_{CC}(\varepsilon_A, \varepsilon_B) = \tau_{DC}(\varepsilon_A, \varepsilon_B) = 0$ and $\tau_{CD}(\varepsilon_A, \varepsilon_B) > 0$.

Clearly $\varepsilon_A \neq 0$ and $\varepsilon_B \neq 0$ Then:

$$\begin{aligned}
\pi_A(\varepsilon_A, \varepsilon_B) &= \tau_{CD} \left[\left(1 - \frac{\varepsilon_A}{2}\right) \left(\left(1 - \frac{\varepsilon_B}{2}\right) \cdot g + \frac{\varepsilon_B}{2} \cdot 2g \right) + \frac{\varepsilon_A}{2} \left(\left(1 - \frac{\varepsilon_B}{2}\right) \cdot 2 + \frac{\varepsilon_B}{2} (2 + g) \right) \right] \\
&\quad + \tau_{DD} \left[\left(1 - \frac{\varepsilon_A}{2}\right) \left(\left(1 - \frac{\varepsilon_B}{2}\right) \cdot 2 + \frac{\varepsilon_B}{2} \cdot (2 + g) \right) + \frac{\varepsilon_A}{2} \left(\left(1 - \frac{\varepsilon_B}{2}\right) \cdot g + \frac{\varepsilon_B}{2} \cdot 2g \right) \right] \\
&< \left(1 - \frac{\varepsilon_A}{2}\right) \left(\left(1 - \frac{\varepsilon_B}{2}\right) \cdot 2 + \frac{\varepsilon_B}{2} \cdot (2 + g) \right) + \frac{\varepsilon_A}{2} \left(\left(1 - \frac{\varepsilon_B}{2}\right) \cdot g + \frac{\varepsilon_B}{2} \cdot 2g \right) \\
&< \left(1 - \frac{\varepsilon_B}{2}\right) \cdot 2 + \frac{\varepsilon_B}{2} (2 + g),
\end{aligned} \tag{67}$$

where the last quantity is attainable by setting $\varepsilon_A = 0$. \square

B Methodology of numerical simulations

B.1 Time heatmaps and payoff functions

In order to get the time spent in each region $\omega_{X,Y}$, we simulate the Q-learning algorithms over $T = 10^5$ periods for every triplet of parameters $(g, \varepsilon_A, \varepsilon_B)$ on a grid of size $64 \times 64 \times 64$. Q-values for the last $T' = 1000$ periods are saved, which allows to deduce which region algorithms are in over this period of time. This process is reproduced $k = 100$ times, and results on the share of time spent in each region are averaged over all the runs. Using the same simulations, we get the transitions happening between regions as presented in Sec. 6.4.

Using the measured share of time spent in each ω_{XY} , we then compute the payoffs associated to each triplet of parameters with the formula given in Sec. 3.5 (equation 15). This allows to get, for each g on the grid, a payoff matrix of size (64×64) . We chose to generate payoff matrices using this method rather than to get them directly from the simulations in order to minimize noise in the results, however both method return similar results (with, indeed, more noise when payoffs are measured directly). Note that this method allows for interpolation: assuming the variation of τ_{XY} with respect to ε_A and ε_B is low enough, we can use the results obtained on the $64 \times 64 \times 64$ grid to interpolate the payoff function.

B.2 Equilibria

Once payoff matrices are generated for each g , we compute best response function. Doing so, we take the mere assumption that best responses are single-valued (which our simulations confirm). At this stage, a best response function is a (finite) list giving, for each ε_B , the best response ε_A^* of player A . We then interpolate this list and generate best response functions as a collection of linear functions (between each ε_B on the grid). For a given g , the best response function is stored as a list of couples (a, b) characterizing the best response function between two ε_B s on the grid. This allows to then construct the symmetric of the curve of the best response function with respect to the 45 line, and to subsequently find Nash equilibria as a profile $(\varepsilon_A, \varepsilon_B)$ lying at the intersection of the best response function and its symmetric. This method allows us to get Fig. 6's left panel.⁶

B.3 Denoised equilibria

The aforementioned method generates a noisy outcome since the τ_{XY} s are generated by a noisy process. We thus would like to distinguish the equilibria appearing because of noise from the others. For this purpose, we generate $M = 1000$ new observations for each $\tau_{XY}^g(\varepsilon_A, \varepsilon_B)$ by randomly adding noise to the originally obtained τ_{XY} s. To generate each new observation, for

⁶This method can of course be used since $G(g)$ is a symmetric game.

each triplet of parameters, we pick a region at random and increase the time spent inside by $\eta = 0.005$, and then pick another region at random and decrease the time spent inside by $-\eta$.⁷ This process generates M new tables of time spent in each region for each triplet of parameters, which are used to generate the same number of payoff matrices. By using the same process as previously described on each of these payoff matrices, we are able to get M new lists of equilibria (one per perturbed table). To obtain Fig. 6's right panel, we let (g, ε) on a (64×64) grid. For (k, m) on the grid, denote g_k and ε_m the corresponding values of g and ε . In each cell (k, m) we represent the frequency with which there is a Nash equilibrium in the game $G(g_k)$ with perturbed payoffs lying between ε_k and ε_{k+1} . This method aims thus allows to get where equilibria are most likely to be found and to de-noise our previously obtained results.

⁷We pick among the regions that allow for such increase (resp. decrease), namely those for which τ_{XY} is below $1 - \eta$ (resp. above η).

C Detection of spontaneous coupling: method

In order to detect spontaneous coupling and measure its basin of attraction, we rely on the position of Q-values in the four-dimensional space $(Q_C^A, Q_D^A, Q_C^B, Q_D^B)$ after a large enough number of periods. In Fig. 7 we plot the projection of the position of the system on a plane for $K = 1000$ different initial conditions uniformly drawn at random in \mathbb{I} : a red dot corresponds to the position of player's B Q-values for one initial condition, while a blue dot corresponds to that of player A . The black lines correspond to values $\frac{2}{1-\gamma}$ and $\frac{2g}{1-\gamma}$, for which Q_C can be above Q_D . On the first panel ($g = 1.7, \varepsilon_A = \varepsilon_B = 0.1$), we clearly see that two clusters exist. The one on the top right part of the figure corresponds to the spontaneous coupling being reached, while the second corresponds to the system reaching $\tilde{Q}_{DD}^{\text{eq}}$. The simple idea behind our measuring the basin of attraction of spontaneous coupling relies on automatically detecting those clusters and measuring their sizes. In order to do so, we use a simple K-means algorithm with $K = 2$, let it detect the clusters and label the points accordingly.⁸

It is important to note that K-means requires the number of clusters to be set in advance, and thus cannot by itself find the optimal number of clusters to perform its task. In our case, this causes issues for two cases. The first case is the one in which spontaneous coupling does not exist and thus only one cluster can be found (corresponding to $\tilde{Q}_{DD}^{\text{eq}}$). The second panel of Fig. 7 shows an example where this happens. The second case is the one in which convergence to $\tilde{Q}_{DD}^{\text{eq}}$ do not show up in our experiments, so that in this case too, only one cluster appears (see the third panel of Fig. 7 for an example). If we were to try and measure the size of the basin of attraction of spontaneous coupling in those cases, the K-means algorithm would identify two clusters of equal size and thus give us a wrong measure. In order to circumvent this difficulty, we perform two additional clustering tasks using K-means algorithms with $K = 2$. The first one aims at identifying the parameters which allows for spontaneous coupling. For this purpose, we use the time spent in ω_{CC} as a feature and run a K-means algorithm in one dimension. Since we know the results should display two clusters (i.e. allowing for spontaneous coupling or not allowing for spontaneous coupling) there is no problem in fixing beforehand the number of clusters to be 2. Doing so, we successfully identify parameters allowing for spontaneous coupling, and for those who don't, we fix the measure of the basin to be 0. We then proceed to perform the clustering task we previously described, and get two features out of it. First, we get the inertia metric associated to this task's outcome as well as the inertia metric associated to the trivial task with $K = 1$ and compute their difference. Second, we get the distance between the identified clusters' centers. We use those two features to perform yet another K-means clustering with $K = 2$ on the parameters allowing for spontaneous coupling⁹. The idea is the

⁸Note that we perform this task in the 4-dimensional space, not in the plane that we use for representation purposes only.

⁹We actually pass the first feature into a sigmoid function allowing to better the clustering by reducing its dependence to extreme values.

following: when the distance between clusters' centers and the difference in the inertia metric are high, this reveals that two clusters exist in the 4-dimensional space, while when they are small, only one cluster should be considered. For parameters belonging to this category, we fix the size of the basin of attraction to 1 and consider the $\tilde{Q}_{DD}^{\text{eq}}$ equilibrium to be reached for a negligible fraction of initial conditions.

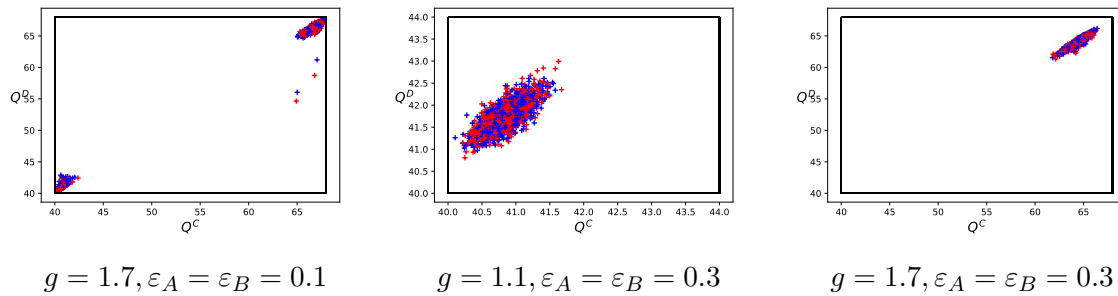


Figure 7: Projection on a plane of the position of the system in the 4 dimensional space

D Generalization to admissible policy functions

In the following we consider a Prisoner's dilemma the payoff of which are given by $\tilde{\pi}_{X,Y}$, with $X, Y \in \{C, D\}$. We consider **policy functions** i.e. functions mapping Q-values into probabilities to play each action and focus on the **admissible** policy functions. For $X \in \{C, D\}$, we denote $\phi_X(\mathbb{Q})$ the probability to play action X when holding Q-values $\mathbb{Q} = (Q_C, Q_D)$, so that $\phi(\mathbb{Q}) = (\phi_C(\mathbb{Q}), \phi_D(\mathbb{Q}))$. We consider a similar game than previously, denoted \mathcal{G} , such that player A chooses its policy function in $\mathcal{A}_A \cup \{greedy\}$ player B chooses from $\mathcal{A}_B \cup \{greedy\}$, where \mathcal{A}_A and \mathcal{A}_B are subsets of admissible policy functions. On top of their policy functions, players choose their learning rates, α , in $]0, 1[$ and their initial conditions in $\mathbb{I} = [\frac{\tilde{\pi}_{CC}}{1-\gamma}, \frac{CD}{1-\gamma}] \times [\frac{\tilde{\pi}_{CD}}{1-\gamma}, \frac{DD}{1-\gamma}]$.

Definition C.1. $\phi : \mathbb{R}^2 \mapsto \Delta(\mathbb{R}^2)$ is an **admissible policy function** if and only if:

- $\forall \mathbb{Q} \in \mathbb{R}^2, \phi(\mathbb{Q}) \in \Delta(\mathbb{R}^2)^*$.
- For all $X, Y \in \{C, D\}$ ϕ is Lipschitz-continuous on $\omega_{X,Y}$.
- For $X \in \{C, D\}$, $\phi_X(\mathbb{Q})$ is increasing in Q_X .
- $\forall \mathbb{Q}, Q_C = Q_D \implies \phi_C(\mathbb{Q}) = \phi_D(\mathbb{Q})$.

Those assumptions guarantee that any admissible policy function features some exploration (we exclude locally greedy policy functions), is smooth enough in each continuity domain so as to be able to define the continuous time approximations and satisfies two reasonable assumptions: they are increasing (in the sense that if we increase one action's Q-value and keep the other constant we increase its probability of being selected) and there's no bias towards a specific action (when Q-values are equal, actions are indistinguishable).

Lemma C.1. Let ϕ an admissible policy function. Then, there exists $\underline{\phi} > 0$ such that:

$$\forall \mathbb{Q} \in \mathbb{I} \equiv [\frac{\pi_{C,D}}{1-\gamma}, \frac{\pi_{C,C}}{1-\gamma}] \times [\frac{\pi_{D,D}}{1-\gamma}, \frac{\pi_{D,C}}{1-\gamma}], \forall X \in \{C, D\}, \phi_X(\mathbb{Q}) \geq \underline{\phi}. \quad (68)$$

Proof. For any $X \in \{C, D\}$, ϕ is Lipschitz-continuous on $\omega_{X,Y}$, thus it is Cauchy-continuous on $\omega_{X,Y}$. As a consequence, we can define $\tilde{\phi}_X : \bar{\omega}_{X,Y} \equiv \omega_{X,Y} \cup \{\mathbb{Q} \in \mathbb{R}^2 \text{ s.t. } Q_C = Q_D\} \mapsto [0, 1]$ to be the continuous extension of ϕ_X on $\omega_{X,Y} \cup \{\mathbb{Q} \in \mathbb{R}^2 \text{ s.t. } Q_C = Q_D\}$. Weierstrass theorem guarantees that there exists $\underline{\phi}_X \equiv \min_{\mathbb{Q} \in \bar{\omega}_{X,Y} \cap \mathbb{I}} \tilde{\phi}_X(\mathbb{Q}) > 0$. Taking $\underline{\phi} = \min(\min_X \underline{\phi}_X, \frac{1}{2})$ yields the result. \square

In the following, A uses (admissible) policy function ϕ^A and B uses (admissible) policy function ϕ^B .

Proposition C.1. *The continuous time approximation in $\omega_{X,Y}$ for A is well-defined and solves:*

$$\begin{cases} \dot{\tilde{Q}}_A^X(t) = \alpha \phi_X^A(\tilde{Q}_A(t)) \left[\sum_{Y \in \{C,D\}} \tilde{\pi}_{X,Y} \phi_Y^B(\tilde{Q}_B(t)) - (1-\gamma) \tilde{Q}_A^X(t) \right] \\ \dot{\tilde{Q}}_A^{-X}(t) = \alpha \phi_{-X}^A(\tilde{Q}_A(t)) \left[\sum_{Y \in \{C,D\}} \tilde{\pi}_{-X,Y} \phi_Y^B(\tilde{Q}_B(t)) - \tilde{Q}_A^{-X}(t) + \gamma \tilde{Q}_A^X(t) \right]. \end{cases} \quad (69)$$

Proof. This result is a direct consequence of Banchio and Mantegazza (2023) Theorem 1. \square

Proposition C.2. *\tilde{Q} has no steady-state in $\omega_{CC} \cup \omega_{CD} \cup \omega_{DC}$.*

Proof. Assume such steady state exists. Then, for $X \in \{C, D\}$ by setting the flow in $\omega_{C,X}$ to 0 we get:

$$\begin{cases} \tilde{Q}_A^{C,ss} = \frac{1}{1-\gamma} \sum_{Y \in C,D} \tilde{\pi}_{C,Y} \phi_Y^B(\tilde{Q}_B(t)) \\ \tilde{Q}_A^{D,ss} = \frac{1}{1-\gamma} \sum_{Y \in \{C,D\}} \phi_Y^B(\tilde{Q}_B(t)) \left[\gamma \tilde{\pi}_{C,Y} + (1-\gamma) \tilde{\pi}_{D,Y} \right] \end{cases} \quad (70)$$

so that $\tilde{Q}_A^{D,ss} > \tilde{Q}_A^{C,ss}$, which gives a contradiction. \square

Proposition C.3. *A steady-state exists in ω_{DD} .*

Proof. $\mathbb{Q} = (Q_C^A, Q_D^A, Q_C^B, Q_D^B)$ is a steady-state in ω_{DD} if and only if:

$$\begin{cases} \tilde{Q}_A^{C,ss} = \frac{1}{1-\gamma} \sum_{Y \in C,D} \tilde{\pi}_{D,Y} \phi_Y^B(\tilde{Q}_{B,ss}) \\ \tilde{Q}_A^{D,ss} = \frac{1}{1-\gamma} \sum_{Y \in \{C,D\}} \phi_Y^B(\tilde{Q}_{B,ss}) \left[\gamma \tilde{\pi}_{D,Y} + (1-\gamma) \tilde{\pi}_{C,Y} \right] \\ \tilde{Q}_B^{C,ss} = \frac{1}{1-\gamma} \sum_{Y \in C,D} \tilde{\pi}_{Y,D} \phi_Y^A(\tilde{Q}_{A,ss}) \\ \tilde{Q}_B^{D,ss} = \frac{1}{1-\gamma} \sum_{Y \in \{C,D\}} \phi_Y^A(\tilde{Q}_{A,ss}) \left[\gamma \tilde{\pi}_{Y,D} + (1-\gamma) \tilde{\pi}_{Y,C} \right] \end{cases} \quad (71)$$

that is if a fixed point exists in ω_{DD} for the following mapping

$$\psi : \mathbb{Q} \mapsto \begin{pmatrix} \frac{1}{1-\gamma} \sum_{Y \in C,D} \tilde{\pi}_{D,Y} \phi_Y^B(\tilde{Q}_B) \\ \frac{1}{1-\gamma} \sum_{Y \in \{C,D\}} \phi_Y^B(\tilde{Q}_B) \left[\gamma \tilde{\pi}_{D,Y} + (1-\gamma) \tilde{\pi}_{C,Y} \right] \\ \frac{1}{1-\gamma} \sum_{Y \in C,D} \tilde{\pi}_{Y,D} \phi_Y^A(\tilde{Q}_A) \\ \frac{1}{1-\gamma} \sum_{Y \in \{C,D\}} \phi_Y^A(\tilde{Q}_A) \left[\gamma \tilde{\pi}_{Y,D} + (1-\gamma) \tilde{\pi}_{Y,C} \right] \end{pmatrix}, \quad (72)$$

where ψ is a continuous mapping from $\omega_{DD} \cap \mathbb{I}$. Consider $\tilde{\psi}$ the following extension of ψ on $\omega_{DD} \cap \bar{\omega}_{DD}$

$$\tilde{\psi} : \mathbb{Q} \mapsto \begin{pmatrix} \frac{1}{1-\gamma} \sum_{Y \in C,D} \tilde{\pi}_{D,Y} \tilde{\phi}_Y^B(\tilde{Q}_B) \\ \frac{1}{1-\gamma} \sum_{Y \in \{C,D\}} \tilde{\phi}_Y^B(\tilde{Q}_B) \left[\gamma \tilde{\pi}_{D,Y} + (1-\gamma) \tilde{\pi}_{C,Y} \right] \\ \frac{1}{1-\gamma} \sum_{Y \in C,D} \tilde{\pi}_{Y,D} \tilde{\phi}_Y^A(\tilde{Q}_A) \\ \frac{1}{1-\gamma} \sum_{Y \in \{C,D\}} \tilde{\phi}_Y^A(\tilde{Q}_A) \left[\gamma \tilde{\pi}_{Y,D} + (1-\gamma) \tilde{\pi}_{Y,C} \right] \end{pmatrix}, \quad (73)$$

where for $P \in \{A, B\}$ and $Y \in \{C, D\}$, $\tilde{\phi}_Y^P$ denotes the previously defined continuous extension of ϕ_Y^P . Clearly, $p\tilde{si}$ is a continuous function from $(\omega_{DD} \cap \bar{\omega}_{DD}) \cap \mathbb{I}$ to itself, which is compact and convex. Applying Brouwer's fixed point theorem guarantees the existence of a steady point in $(\omega_{DD} \cap \bar{\omega}_{DD})$. Denote it Q^{ss} and assume it is such that $Q_C^{A,ss} = Q_D^{A,ss}$ or $Q_C^{B,ss} = Q_D^{A,ss}$. This immediately gives a contradiction similar to the previous proposition's proof. Thus, a fixed point exists in $\omega_{DD} \cap \mathbb{I}$. \square

Definition C.2. $(\phi_A, \phi_B, \alpha, \tilde{\pi})$ *allows for spontaneous coupling* if and only if there exists $Q_0 \in \mathbb{I}$ such that:

$$\forall S \subset \mathbb{R}^4 \text{ s.t. } \mathbb{P}(\exists t \in \mathbb{N}, Q_t \in S) = 1, \exists \tilde{Q}_0 \in S, \neg \left(\lim_{+\infty} \tilde{Q}_t(\phi_A, \phi_B, \alpha_A, \alpha_B, \tilde{\pi}, \tilde{Q}_0) \in \omega_{DD} \right). \quad (74)$$

Lemma C.2. *If for some player P , $\forall t, \phi_X(\tilde{Q}_P(t)) = \phi_X(\tilde{Q}_X(0))$, then the continuous time approximation of $-P$ cannot stay in ω_C^{-P} . More formally:*

$$\exists t \in \mathbb{R} \text{ s.t. } \tilde{Q}_{-P}(t') \in \omega_D \quad (75)$$

Proof. Take $P = A$ and $-P = B$ without loss of generality. Let $t \in \mathbb{R}$ such that $Q_B(t') \in \omega_C^B$. Then:

$$\dot{Q}_B^C(t) = \alpha \phi_C^B(Q_B(t)) \left[\sum_{Y \in \{C, D\}} \phi_Y^X(0) \tilde{\pi}_{C,Y} - (1 - \gamma) Q_B^C(t) \right]. \quad (76)$$

We first show the latter has constant sign, which amounts to showing that:

$$f(t) \equiv \sum_{Y \in \{C, D\}} \phi_Y^X(0) \tilde{\pi}_{C,Y} - (1 - \gamma) Q_B^C(t) \quad (77)$$

has constant sign. Assume it does not, in particular assume there exists $t_1, t_2 \in \mathbb{R}$ such that $f(t_1) < 0$ and $f(t_2) > 0$. Then, by continuity of f , and the intermediate value theorem, there exists t^* such that $f(t^*) = 0$. Since f is \mathcal{C}^1 , the mean value theorem guarantees that there exists $t' \in]t^*, t_2[$ such that $f'(t') > 0$. Assume that for each such t' , $f(t') \leq 0$. Now we construct the following sequence recursively:

$$\begin{cases} t_0 = \min_{]t^*, t_2[} \left(\{t' \text{ s.t. } f'(t') > 0\} \right) \\ \forall n \in \mathbb{N}^*, t_n = \max_{]t_{n-1}, t_2[} \left(\{t'' \text{ s.t. } f'(t'') > 0\} \right), \end{cases} \quad (78)$$

where our hypothesis and the mean value theorem guarantees $(t_n)_{n \in \mathbb{N}}$ is well-defined. Observe that we can construct $(t_n)_{n \in \mathbb{N}}$ in such a way that $\lim_{+\infty} t_n = t_2$. Indeed, assume that $\bar{t} \equiv \sup_{n \in \mathbb{N}} t_n < t_2$, then, since $(t_n)_{n \in \mathbb{N}}$ is increasing and bounded above, it converges to \bar{t} . Note

also that for all $n \in \mathbb{N}$, $f'(t_n) > 0$ and $f(t_n) \leq 0$, so that, by f being \mathcal{C}^1 :

$$f(\bar{t}) = f(\lim_{+\infty}(t_n)) = \lim_{+\infty} f(t_n) \leq 0, \quad (79)$$

so that applying the mean value theorem once again yields

$$\exists \bar{t}' \in]\bar{t}, t_2[\text{ such that } f'(\bar{t}') \geq 0, \quad (80)$$

so that we can construct another sequence $\tilde{t}_{n \in \mathbb{N}}$ that is not bounded above by \bar{t} . But then:

$$0 \leq \lim_{+\infty} f(t_n) = f(t_2) > 0, \quad (81)$$

which gives a contradiction. Then, there exists $t \in]t^*, t'[$ such that $f'(t) > 0$ and $f(t) > 0$, which contradicts the definition of f . The case in which $f(t_1) > 0$ and $f(t_2) < 0$ can be treated symmetrically. Thus we conclude that f , and thus \dot{Q}_B^C does not change sign. Assume \dot{Q}_B^C remains positive, then:

$$\dot{Q}_B^C(t) \leq \alpha \bar{\phi}_C^B \left[\sum_{Y \in \{C, D\}} \phi_Y^X(0) \tilde{\pi}_{C, Y} - (1 - \gamma) Q_B^C(t) \right], \quad (82)$$

so that for some K_0 :

$$Q_B^C(t) \leq K_0 \exp(-\alpha(1 - \gamma) \bar{\phi}_C^B t) + \frac{\sum_{Y \in \{C, D\}} \phi_Y^A(0) \tilde{\pi}_{C, Y}}{1 - \gamma} \xrightarrow{\gamma \rightarrow +\infty} \frac{\sum_{Y \in \{C, D\}} \phi_Y^A(0) \tilde{\pi}_{C, Y}}{1 - \gamma}. \quad (83)$$

Since by hypothesis $\dot{Q}_B^C(t) > 0$, we conclude by the squeeze theorem that $\lim_{+\infty} Q_B^C(t) = \frac{\sum_{Y \in \{C, D\}} \phi_Y^A(0) \tilde{\pi}_{C, Y}}{1 - \gamma}$. Treating symmetrically the case in which $\dot{Q}_B^C(t) < 0$ yields the same result.

Now, consider the Q-value for D and note that:

$$\begin{aligned} \dot{Q}_B(t) &= \alpha \phi_D^B(\tilde{Q}_B(t)) \left[\sum_{Y \in \{C, D\}} \tilde{\pi}_{D, Y} \phi_Y^A(\tilde{Q}_A(0)) - \tilde{Q}_B^D(t) + \gamma \tilde{Q}_B^C(t) \right] \\ &\geq \alpha \phi_D^B(\tilde{Q}_B(t)) \left[\sum_{Y \in \{C, D\}} \tilde{\pi}_{D, Y} \phi_Y^B(\tilde{Q}_B(t)) + (1 - \gamma) \tilde{Q}_B^D(t) \right] \\ &\xrightarrow{\gamma \rightarrow +\infty} \frac{\sum_{Y \in \{C, D\}} \tilde{\pi}_{D, Y} \phi_Y^A(\tilde{Q}_A(0))}{1 - \gamma}, \end{aligned} \quad (84)$$

where the latter limit is found following a similar reasoning than previously. Comparing the two limits obtained yield a contradiction: there exists t such that $Q_B^C(t) < Q_B^D(t)$. \square

Proposition C.4. *For any $\alpha \in]0, 1[$ and $\gamma \in [0, 1]$, if one player uses a greedy algorithm and the other chooses an admissible policy function then no spontaneous coupling is allowed.*

Proof. First we prove that, with probability 1 there exists $t \in \mathbb{N}$ such that for all $t' > t$:

$$Q_A^D(t') > Q_A^C(t'). \quad (85)$$

We prove that any realization that does not satisfy the above property has probability of occurrence equal to 0. First, let a realization such that $\forall t, Q_A^C(t) > Q_A^D(t)$. There exists L such that if B consecutively plays D L times, $Q_A^C(t+L) \leq Q_A^D(t+L) = Q_A^D(0)$. One such realization with length t thus has probability of occurrence less than ϕ_B^{tL} , so that clearly $\mathbb{P}(\forall t, Q_A^C(t) > Q_A^D(t)) = 0$. Now, let a realization with non-zero probability of occurrence such that for all $t \in \mathbb{N}$ there exists $t' > t$ such that $Q_A^C(t) \geq Q_A^D(t)$. Then, for any such t' , $Q_A^C(t) \geq \frac{\tilde{\pi}_{DD}}{1-\gamma}$, so that in case B plays D at t' , $Q_A^C(t'+1) - Q_A^C(t') \leq \alpha(\pi_{CD} - \pi_{DD})$. From the previous argument, there exists $T = \{\tau \in \mathbb{N} \text{ s.t. } Q_A^D(\tau-1) > Q_A^C(\tau-1) \text{ and } Q_A^C(\tau) \geq Q_A^D(\tau-1)\}$, a sequence of moments in time at which Q-values cross, and such that $|T| = +\infty$. Note that $(Q_A^C(\tau))_{\tau \in T}$ is a decreasing sequence (since Q-values remain still when not updated). Using a similar reasoning than previously, since we consider a realization with non-zero probability of occurrence, there exists $\varepsilon > 0$ and $T_\varepsilon \subset T$ such that $(Q_A^C(\tau))_{\tau \in T_\varepsilon}$ and $\forall \tau \in T_\varepsilon, Q_A^C(\tau) - Q_A^C(\tau+1) \leq \varepsilon$. Consequently, $\lim_{\tau \rightarrow \infty} Q_A^C(\tau) = -\infty$, giving a contradiction.

Now we write the continuous time approximation of B when A only plays D :

$$\begin{cases} \dot{Q}_B^X(t) = \alpha \phi_X^A(\tilde{Q}_A(t)) \left[\tilde{\pi}_{X,D} - (1-\gamma)\tilde{Q}_B^X(t) \right] \\ \dot{Q}_B^{-X}(t) = \alpha \phi_{-X}^A(\tilde{Q}_A(t)) \left[\tilde{\pi}_{-X,D} - \tilde{Q}_B^{-X}(t) + \gamma\tilde{Q}_B^X(t) \right]. \end{cases} \quad (86)$$

By contradiction, assume that for all $t \in \mathbb{R}$ there exists t' such that $\tilde{Q}_B^{-X}(t') \in \omega_C^B$. Note that, for any $X \in \{C, D\}$ and for all $t \in \mathbb{R}$, $\dot{Q}_B^X(t) < 0$ when X is the preferred action. Then following a reasoning similar than the first part of the proof, we get that $\tilde{Q}_B^C(t)$ eventually gets below $\tilde{\pi}_{D,D}$, which completes the proof. \square

Proposition C.5. *For all $\alpha_A, \alpha_B \in]0, 1[$, $(\text{greedy}, \text{greedy})$ allows for spontaneous coupling. More precisely, either there exists t such that for any $t' > t$ $\tilde{Q}(t) \in \omega_{CC}$ or exists t such that for any $t' > t$ $\tilde{Q}(t) \in \omega_{DD}$.*

Proof. In this specific case, only the action with the highest Q-value is played and it increases if and only if the other player plays C . As a consequence, ω_{CC} is absorbing in the sense that whenever $\tilde{Q}(t) \in \omega_{CC}$, then for all subsequent t' , $\tilde{Q}(t') \in \omega_{CC}$. In particular, any initial condition in ω_{CC} causes the system to remain in ω_{CC} ¹⁰. Assume now that:

$$\forall t, \exists t' > t \text{ s.t. } \tilde{Q}(t) \notin \omega_{CC}, \quad (87)$$

¹⁰Note that some initial conditions in $\omega_{CD} \cup \omega_{DC} \cup \omega_{DD}$ leads to ω_{CC} as well.

then using a similar reasoning than for the first part of Proposition 4, we get our result. \square

Proposition C.6. *For all $\alpha_A, \alpha_B \in]0, 1[$ and $\mathbb{Q}(0) \in \omega_{CC}$, $(\text{greedy}, \text{greedy}, \mathbb{Q}(0), \alpha_A, \alpha_B)$ is a Nash equilibrium in \mathcal{G} .¹¹*

Proof. Assume player B plays $(\alpha_B, \text{greedy}, (Q_B^C(0), Q_B^D(0)) \in \omega_C^B)$. We prove that that $(\alpha_A, \text{greedy}, (Q_A^C(0), Q_A^D(0)) \in \omega_C^A)$ is a best response. Take any arbitrary initial condition $(Q_A^C(0), Q_A^D(0))$, then if A use an admissible policy function, then we know by Proposition 4 that no spontaneous coupling is possible. Thus the system ends up in ω_{DD} and B is greedy: thus he only plays D . As a consequence, A is guaranteed to receive payoff strictly less than $\tilde{\pi}_{DD}$. If A uses a greedy algorithm, he gets either $\tilde{\pi}_{CC}$ or $\tilde{\pi}_{DD}$, and thus is strictly better off. As a consequence, any best response for A uses a greedy algorithm. It is then clear that any $(\alpha_A, \text{greedy}, (Q_A^C(0), Q_A^D(0)) \in \omega_C^A)$ is a best response to B 's strategy. \square

Proposition C.7. *Let $(\phi_A, \phi_B, \mathbb{Q}(0), \alpha_A, \alpha_B)$ a Nash equilibrium of \mathcal{G} . Then (ϕ_A, ϕ_B) allows for spontaneous coupling.*

Proof. Let $(\phi_A, \phi_B, \mathbb{Q}(0), \alpha_A, \alpha_B)$ a Nash equilibrium of \mathcal{G} such that (ϕ_A, ϕ_B) does not allow for spontaneous coupling, so that $\tau_{DD}(\phi_A, \phi_B) = 0$. Then A plays C with positive probability, whereas by using a greedy algorithm A , τ_{DD} is equal to 1 as well (Proposition 4) and A plays D with probability 1. Thus, at such Nash equilibrium, A uses a greedy algorithm, but then B best responds with a greedy algorithm as well. However we know that $(\text{greedy}, \text{greedy})$ allows for spontaneous coupling. \square

¹¹Our previous remark concerning initial conditions in $\omega_{CD} \cup \omega_{DC} \cup \omega_{DD}$ leading to ω_{CC} implies the existence of Nash equilibria using initial conditions outside ω_{CC} .

References

- [1] ABADA, I., AND LAMBIN, X. Artificial intelligence: Can seemingly collusive outcomes be avoided? *Management Science* (2023).
- [2] ASKER, J., FERSHTMAN, C., AND PAKES, A. Artificial intelligence, algorithm design, and pricing. *AEA Papers and Proceedings 112* (May 2022), 452–456.
- [3] ASSAD, S., CLARK, R., ERSHOV, D., AND XU, L. Algorithmic pricing and competition: Empirical evidence from the german retail gasoline market. *SSRN Electronic Journal* (2020).
- [4] BANCHIO, M., AND MANTEGAZZA, G. Adaptive algorithms and collusion via coupling, 2022.
- [5] BANCHIO, M., AND SKRZYPACZ, A. Artificial intelligence and auction design, 2022.
- [6] BANERJEE, D., AND SEN, S. Reaching pareto-optimality in prisoner’s dilemma using conditional joint action learning. *Autonomous Agents and Multi-Agent Systems 15* (2007), 91–108.
- [7] CALVANO, E., CALZOLARI, G., DENICOLÒ, V., AND PASTORELLO, S. Algorithmic pricing what implications for competition policy? *Review of Industrial Organization 55*, 1 (Feb. 2019), 155–171.
- [8] CALVANO, E., CALZOLARI, G., DENICOLÒ, V., AND PASTORELLO, S. Artificial intelligence, algorithmic pricing, and collusion. *American Economic Review 110*, 10 (Oct. 2020), 3267–3297.
- [9] CALVANO, E., CALZOLARI, G., DENICOLÓ, V., AND PASTORELLO, S. Algorithmic collusion with imperfect monitoring. *International Journal of Industrial Organization 79* (Dec. 2021), 102712.
- [10] CANESE, L., CARDARILLI, G. C., DI NUNZIO, L., FAZZOLARI, R., GIARDINO, D., RE, M., AND SPANÒ, S. Multi-agent reinforcement learning: A review of challenges and applications. *Applied Sciences 11*, 11 (2021), 4948.
- [11] COLLIARD, J.-E., FOUCAULT, T., AND LOVO, S. Algorithmic pricing and liquidity in securities markets. *HEC Paris Research Paper* (2022).
- [12] COMPTE, O. Q-based equilibria, 2023.
- [13] DIECI, L., ELIA, C., AND LOPEZ, L. A filippov sliding vector field on an attracting co-dimension 2 discontinuity surface, and a limited loss-of-attractivity analysis, Feb 2013.

- [14] DIECI, L., AND LOPEZ, L. Sliding motion on discontinuity surfaces of high co-dimension. a construction for selecting a filippov vector field, Feb 2011.
- [15] DOLGOPOLOV, A. Reinforcement learning in a prisoner’s dilemma. *Games and Economic Behavior* 144 (2024), 84–103.
- [16] FILIPPOV, A. F. Differential equations with discontinuous right-hand side. *Matematicheskii sbornik* 93, 1 (1960), 99–128.
- [17] FORGY, E. W. Cluster analysis of multivariate data: efficiency versus interpretability of classifications. *biometrics* 21 (1965), 768–769.
- [18] HETTICH, M. Algorithmic collusion: Insights from deep learning. *Available at SSRN* 3785966 (2021).
- [19] HU, J., AND WELLMAN, M. P. Nash q-learning for general-sum stochastic games. *Journal of machine learning research* 4, Nov (2003), 1039–1069.
- [20] JOHNSON, J. P., RHODES, A., AND WILDENBEEST, M. Platform design when sellers use pricing algorithms. *Econometrica* 91, 5 (2023), 1841–1879.
- [21] KENNEDY, J., AND EBERHART, R. Particle swarm optimization. In *Proceedings of ICNN’95-international conference on neural networks* (1995), vol. 4, IEEE, pp. 1942–1948.
- [22] KIANERCY, A., AND GALSTYAN, A. Dynamics of boltzmann q learning in two-player two-action games. *Physical Review E* 85, 4 (2012), 041145.
- [23] KLEIN, T. Autonomous algorithmic collusion: Q-learning under sequential pricing. *The RAND Journal of Economics* 52, 3 (Aug. 2021), 538–558.
- [24] LERER, A., AND PEYSAKHOVICH, A. Maintaining cooperation in complex social dilemmas using deep reinforcement learning. *arXiv preprint arXiv:1707.01068* (2017).
- [25] LLOYD, S. Least squares quantization in pcm. *IEEE transactions on information theory* 28, 2 (1982), 129–137.
- [26] MASKIN, E., AND TIROLE, J. A theory of dynamic oligopoly, ii: Price competition, kinked demand curves, and edgeworth cycles. *Econometrica: Journal of the Econometric Society* (1988), 571–599.
- [27] MNIH, V., KAVUKCUOGLU, K., SILVER, D., RUSU, A. A., VENESS, J., BELLEMARE, M. G., GRAVES, A., RIEDMILLER, M., FIDJELAND, A. K., OSTROVSKI, G., ET AL. Human-level control through deep reinforcement learning. *nature* 518, 7540 (2015), 529–533.

- [28] MUSOLFF, L. Algorithmic pricing facilitates tacit collusion. In *Proceedings of the 23rd ACM Conference on Economics and Computation* (July 2022), ACM.
- [29] NOWÉ, A., VRANCX, P., AND DE HAUWERE, Y.-M. Game theory and multi-agent reinforcement learning. *Reinforcement Learning: State-of-the-Art* (2012), 441–470.
- [30] SANCHEZ-CARTAS, J. M., AND KATSAMAKAS, E. Artificial intelligence, algorithmic competition and market structures. *IEEE Access* 10 (2022), 10575–10584.
- [31] TAMPUU, A., MATHISEN, T., KODELJA, D., KUZOVKIN, I., KORJUS, K., ARU, J., ARU, J., AND VICENTE, R. Multiagent cooperation and competition with deep reinforcement learning. *PLOS ONE* 12, 4 (Apr. 2017), e0172395.
- [32] TESAURO, G. Extending q-learning to general adaptive multi-agent systems. *Advances in neural information processing systems* 16 (2003).
- [33] WATKINS, C. J., AND DAYAN, P. Q-learning. *Machine learning* 8 (1992), 279–292.
- [34] XU, Z., AND ZHAO, W. On mechanism underlying algorithmic collusion. *arXiv preprint arXiv:2409.01147* (2024).